Chemical Science

ROYAL SOCIETY OF CHEMISTRY

PERSPECTIVE

View Article Online
View Journal | View Issue

Cite this: *Chem. Sci.*, 2020, **11**, 12974

All publication charges for this article have been paid for by the Royal Society of Chemistry

Received 3rd September 2020
Accepted 14th November 2020

DOI: 10.1039/d0sc04881j

rsc.li/chemical-science

C–H functionalization reactions enabled by hydrogen atom transfer to carbon-centered radicals

Sumon Sarkar, † Kelvin Pak Shing Cheung † and Vladimir Gevorgyan *

Selective functionalization of ubiquitous unactivated C–H bonds is a continuous quest for synthetic organic chemists. In addition to transition metal catalysis, which typically operates under a two-electron manifold, a recent renaissance in the radical approach relying on the hydrogen atom transfer (HAT) process has led to tremendous growth in the area. Despite several challenges, protocols proceeding *via* HAT are highly sought after as they allow for relatively easy activation of inert C–H bonds under mild conditions leading to a broader scope and higher functional group tolerance and sometimes complementary reactivity over methods relying on traditional transition metal catalysis. A number of methods operating *via* heteroatom-based HAT have been extensively reported over the past few years, while methods employing more challenging carbon analogues have been less explored. Recent developments of mild methodologies for generation of various carbon-centered radical species enabled their utilization in the HAT process, which, in turn, led to the development of remote C(sp^3)–H functionalization reactions of alcohols, amines, amides and related compounds. This review covers mostly recent advances in C–H functionalization reactions involving the HAT step to carbon-centered radicals.

Introduction

Selective functionalization of C–H bonds in organic molecules is highly desirable as this atom- and step-economic approach allows for late stage functionalization and diversification of complex molecules, and sometimes previously unattainable unique retrosynthetic disconnections.[1] However, selective and efficient functionalization of ubiquitous C–H bonds is a highly challenging task due to the inertness of these bonds, and also lack of control for activation of a specific C–H site among other similar C–H bonds available.[2]

Over the past decades, transition metal-catalyzed C–H activation and carbene/nitrene insertion reactions have been developed tremendously (Scheme 1a).[3] However, these methods typically require high temperature conditions, as well as directing groups, some of which are not removable. The selectivity of C–H activation mostly depends on thermodynamic stability of the resultant carbon–metal species. Thus, primary C–H sites are easier to activate compared to their secondary counterparts, while activation of tertiary C–H bonds is rare. On the other hand, carbene and nitrene insertion reactions occur preferentially at the most electron-rich C–H bonds. Nonetheless, steric influence can be the dominant factor in some cases. Moreover, these processes usually employ diazo compounds or amides to access the corresponding metal carbene and metal nitrene species. An electron withdrawing group such as an ester (*i.e.* α-diazo ester) is often required, thus limiting the choice of reaction substrates.

In contrast, hydrogen atom transfer (HAT)[4] represents an alternative approach toward C–H functionalization. Since HAT is highly influenced by bond dissociation energy (BDE), for a given system, HAT from tertiary C–H sites is faster than that from secondary and primary positions. Thus, methods relying on HAT exhibit a selectivity trend complementary to that for two-electron transition metal-catalyzed approaches.[5]

The HAT process has long been recognized as a versatile tool for C–H functionalization due to its high reactivity and regioselectivity. Historic precedence of 1,5-HAT initiated by nitrogen- and oxygen-centered radicals was showcased in the Hofmann–Löffler–Freytag reaction and Barton's nitrite photolysis.[6] This radical approach discovered in the 19th century, despite being highly regioselective and exergonic, did not make an appearance among the mainstream C–H functionalization methods until mild generation of radicals was developed.[7] Likewise, carbon-centered radical-mediated HAT was first reported in 1954 (ref. 8) and was not utilized in organic synthesis until the late 1980's;[9] however, it has enjoyed rapid employment in synthesis in the past decade.

The rate of HAT is mostly controlled by enthalpic factors; however, the Thorpe–Ingold effect also plays an important role in the case of intramolecular HAT.[10] With few exceptions,[11] HAT proceeds *via* an early transition state due to its exothermic

Department of Chemistry and Biochemistry, University of Texas at Dallas, 800 W Campbell Rd, Richardson, Texas, 75080, USA. E-mail: vlad@utdallas.edu

† These authors contributed equally to this work.

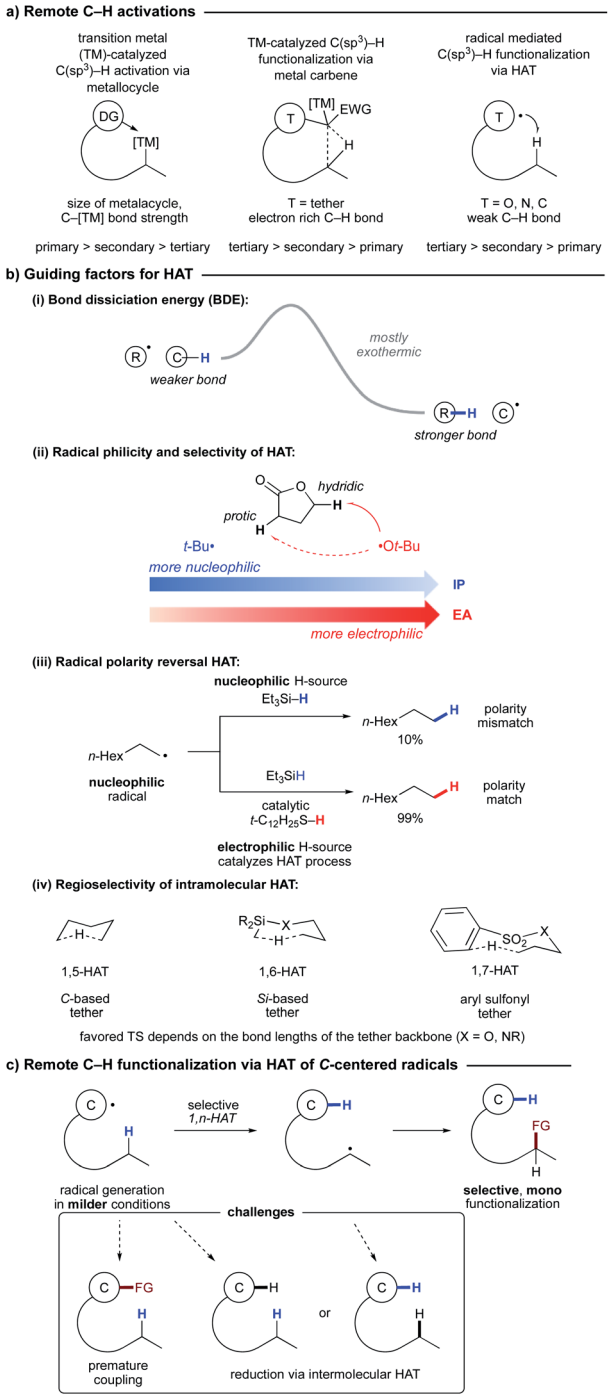

Scheme 1 (a) Different modes of remote C–H functionalization. (b) Guiding factors for HAT. (c) Remote C–H functionalization *via* HAT to C-centered radicals.

nature. Usually aryl, vinyl, or primary alkyl radicals undergo HAT at alkyl C–H sites due to their higher parent C–H BDEs (Scheme 1b(i)). In the case where these BDE differences are comparable, the process can potentially be reversible;[12] thus a selective functionalization becomes more challenging. Another important factor governing the efficiency and selectivity of HAT is radical philicity (polarity).[13] The radical philicity, electrophilicity, or nucleophilicity index can be quantified from the ionization potential (IP) and electron affinity (EA) of free radicals. Given similar BDE differences, an electrophilic radical is expected to undergo HAT preferentially from a more hydridic C–H site and *vice versa* (Scheme 1b(ii)).[4b,14] In case of polarity mismatch, another HAT agent can be used for polarity reversal catalysis (Scheme 1b(iii)).[15]

C-Centered radicals can abstract hydrogen *via* intramolecular 1,*n*-HAT where n = 4–8, or even higher (Scheme 1b(iv)).[7a,b,d–g] The predictable site-selective HAT relies on optimal orientation (linear to quasi-linear: ≤35°) and distance (≤3 Å) between the radical and the H-atom at the abstraction site.[16] Higher activation energy for other intramolecular HATs can be attributed to increased C–H–C strain for 1,3- and 1,4-HAT, or entropic barrier for higher order HATs. However, incorporation of heteroatoms can alter the preferred geometry and thus the site of HAT. For example, a silicon-based tether displays a preference for 1,6-HAT, while an arylsulfonyl tether is predisposed to 1,7-HAT (see below).

Common generation of O- and N-centered radicals for HAT involves single electron reduction of very weak oxygen- or nitrogen-heteroatom bonds or strong oxidants required to oxidize nitrogen or oxygen centers. In contrast, generation of C-centered radicals can now be done under a variety of benign conditions using organic halides, redox-active esters, triflates, and diazonium salts. However, there are a few challenges associated with the C–H functionalization *via* HAT of C-centered radicals (Scheme 1c). Since both the initial and translocated radicals are very similar in nature, there is a possibility of a premature coupling process. However, this problem can be addressed by using radicals of different radical philicities and by matching the polarity of the reagent and translocated radical.[17] In addition, due to lower BDE differences, the rate of HAT to the C-centered radical from the alkyl C–H site can be low, thus competing with other HAT processes, including an unwanted intermolecular HAT process with solvent giving rise to reduction byproducts.

This review covers C–H functionalizations involving HAT to a C-centered radical, with emphasis placed on the theoretical background and challenges of HAT involving C-centered

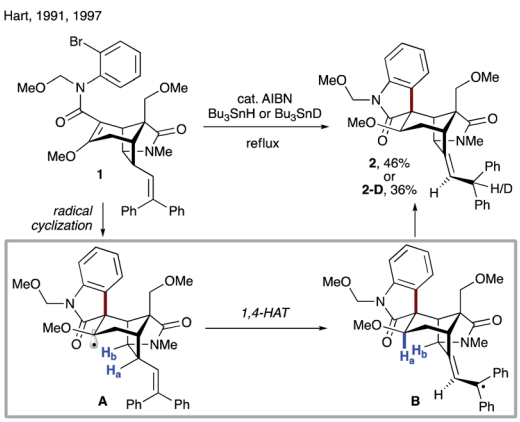

Scheme 2 1,4-HAT in synthetic studies toward gelsemine.

radicals. It should be noted that this topic has been partially covered in several excellent reviews;[5,7a–d] however, since then an increasing number of reports have appeared in the literature. Hence, this review summarizes the progress in this emerging area of HAT, organized by the distance of HAT and type of C-centered radical.

HAT involving alkyl radicals

Intramolecular HAT

1,4-HAT. Literature examples of 1,4-HAT are scarce and typically involve sterically constrained substrates. Hart and co-workers observed oxindole **2** as the major product during their studies toward synthesis of the oxindole fragment of gelsemine (Scheme 2).[18] Use of tributyltin deuteride led to product **2-D**, thus supporting the mechanism in which intermediate **A**, formed upon radical cyclization of bromide **1** in the presence of tributyltin hydride (Bu_3SnH) and azobisisobutyronitrile (AIBN) initiator, undergoes 1,4-HAT to give stable tertiary benzylic radical **B**. In this case, 1,4-HAT is favored by not only the enthalpic factor but also rigidity of **A**, which ensures that the radical center is in close proximity to H_a.

Crich and co-workers showed that 1,4-HAT could be a competitive pathway during the inversion of α- to β-pyranosides *via* 1,5-HAT.[19] As depicted in Scheme 3a, reaction of **3** with Bu_3SnH in the presence of AIBN leads to radical **A**, which can undergo 1,5-HAT, followed by axial HAT, to afford the desired β-mannoside **4** after workup. Alternatively, competing 1,4-HAT can occur, resulting in intermediate **B**. The latter may afford α-mannoside **5** or glucoside **6** *via* HAT, or ketone **7** upon β-scission. The product distribution clearly shows that 1,4-HAT is not only viable but indeed the major pathway in this rigid system. In addition, exclusive formation of ketone **7** was observed when glucoside **8** was used (Scheme 3b).

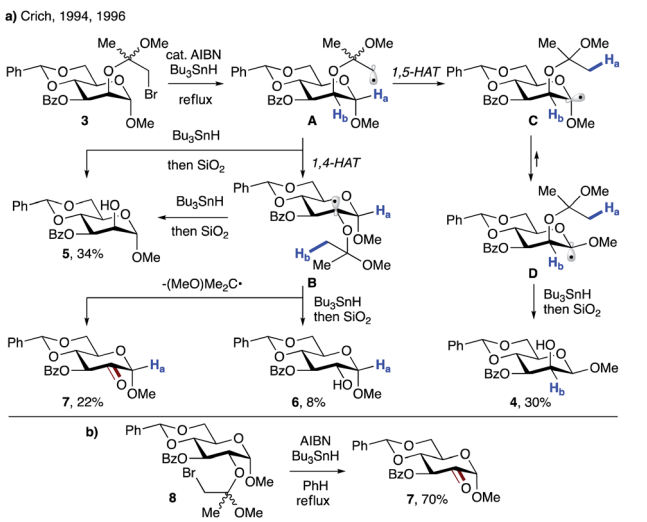

Scheme 3 (a) 1,4-HAT triggered by radical **A** originating from bromoethyl mannoside **3**. (b) Synthesis of ketone **7** by 1,4-HAT/fragmentation of bromoethyl glucoside **8**.

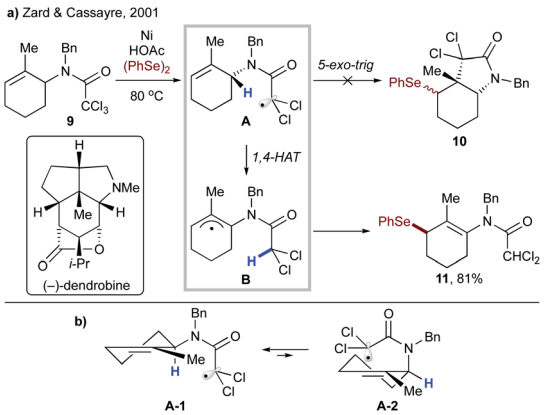

Scheme 4 (a) Formation of cyclic enamide **11** *via* a 1,4-HAT/arylselenation cascade. (b) Conformational analysis of the 1,4-HAT process *vs.* 5-*exo*-*trig* cyclization.

In 2001, Zard and Cassayre reported a short synthesis of (−)-dendrobine,[20] in which the pyrrolidine core was thought to be constructed *via* radical cyclization of the corresponding trichloroacetamide (**9** → **10**, Scheme 4a). However, upon treatment of model substrate **9** with nickel and acetic acid in the presence of diphenyl diselenide, enamide **11** was obtained instead of the anticipated bicyclic lactam **10**. This suggests that 1,4-HAT toward stable allylic radical **B** occurred preferentially over the 5-*exo*-*trig* cyclization. Bertrand, Nechab and co-workers

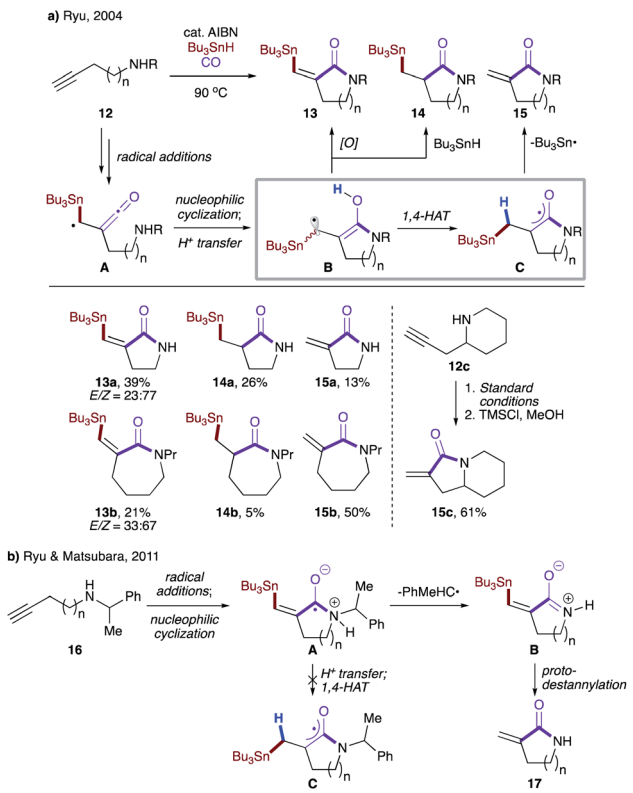

Scheme 5 (a) Rationale for the formation of three products. (b) Phenethyl radical as a leaving group.

provided a plausible explanation based on the conformational analysis of conformers **A-1** and **A-2** leading to 1,4-HAT and 5-*exo-trig* processes, respectively (Scheme 4b).[21]

Ryu and co-workers observed formation of three different products while investigating the reactivity of α-ketenyl radicals with an internal amino group (Scheme 5a).[22a] The reaction begins with radical addition of the tributyltin radical to **12**, followed by trapping of carbon monoxide to give α-ketenyl radical **A**, which then engages in nucleophilic cyclization with a tethered amino group. A subsequent proton transfer affords hydroxylallyl radical **B**, which may either be oxidized to lactam **13**, convert to reduced lactam **14** upon intermolecular HAT with Bu_3SnH, or perform 1,4-HAT to produce intermediate **C**. The latter then extrudes the tributyltin radical to furnish **15**. Alternatively, **15** could be obtained *via* protodestannylation of **13**, as exemplified in the one-pot two-step transformation of **12c** to **15c**. The product distribution varies with the lactam ring size, with larger rings favoring 1,4-HAT over the other two pathways. This was later rationalized by DFT calculations, which showed that despite all being highly exothermic, the activation barrier decreased with ring size (17.0 kcal mol^{-1} for $n = 4$ *vs.* 25.3 kcal mol^{-1} for $n = 1$).[22b] It was also found that in the case of phenethylamines **16**, ejection of the phenethyl radical preceded proton transfer and hence bypassed 1,4-HAT, resulting in intermediate **A**, which was exclusively converted to **B**, which upon treatment with TMSCl afforded lactam **17** (Scheme 5b).

In 2006 and 2008, Dake and co-workers disclosed synthetic routes toward nitiol derivatives **20** (ref. 23) and fusicoccane A–B ring fragment **21** (ref. 24) involving tandem Norrish type 1 fragmentation/1,4-HAT (Scheme 6). First, upon UV irradiation, a photoexcited ketone **18** undergoes fragmentation to form biradical **A**, which after intersystem crossing (ISC) undergoes 1,4-HAT to afford ketene intermediate **B**. Nucleophilic trapping with methanol solvent leads to the key intermediate, ester **19**.

In 2012, the group of Li and Shi reported the synthesis of bicyclo[3.1.0]hexane derivatives **22** *via* radical reaction between vinylidene cyclopropanes and diphenyl diselenide.[25] The vinylcyclopropane moiety of **22** undergoes thermally induced ring-opening, followed by 1,4-HAT, to give biradical **C**, which produces cyclohexene derivatives **23** or **24** (Scheme 7a). In all

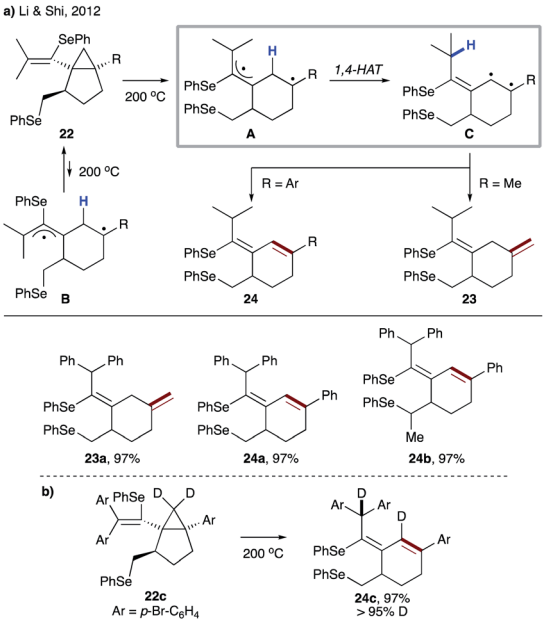

Scheme 7 (a) Thermally induced ring-opening/1,4-HAT cascade transformation of **22**. (b) Evidence for the 1,4-HAT process from a deuterium-labelling experiment.

cases, excellent stereoselectivity was observed, which could be explained by unfavourable formation of the conformer **B**. Involvement of 1,4-HAT in this thermal rearrangement was supported by the reaction of D-labeled substrate **22c**, as well as by DFT calculations (Scheme 7b).

1,5-HAT. Studies toward the chemistry of carbon-to-carbon 1,5-HAT date back to the 1970s. In 1973, Morrison's group revealed that olefin **25** underwent UVC-photoinduced internal exchange between vinyl deuterium and methyl hydrogen (Scheme 8a).[26] UV excitation of **25** generates 1,2-biradical **A**, which undergoes 1,5-HAT to produce *o*-xylylene intermediate **B**, followed by a ground state 1,5-deuterium shift to afford exchanged product **26**. Later, Pratt confirmed the intermediacy of *o*-xylylene in the formation of [4 + 2] adduct **28** with maleic anhydride (Scheme 8b).[27] Similar transformations have also been reported by Hornback.[28]

Very recently, Koert's group reported an interesting example of naphthocyclobutene synthesis from methyl (α-

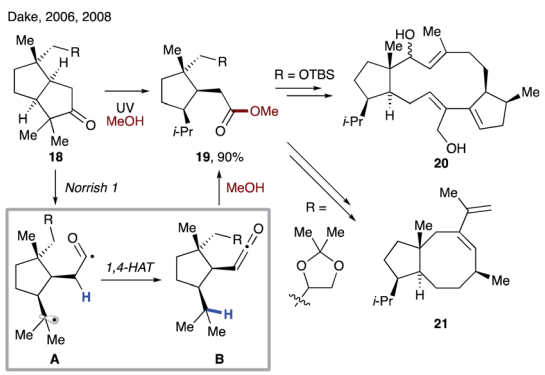

Scheme 6 Synthesis of natural product derivatives **20** and **21** *via* the 1,4-HAT process.

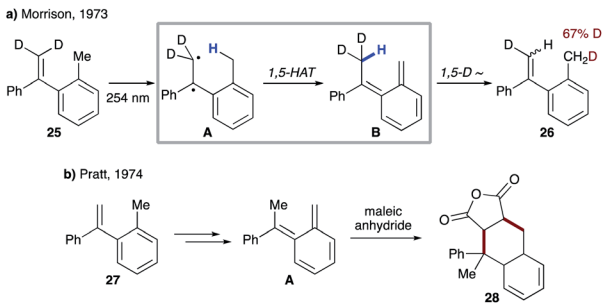

Scheme 8 (a) Photoinduced internal H/D exchange of **25**. (b) Trapping of the *o*-xylylene intermediate with maleic anhydride.

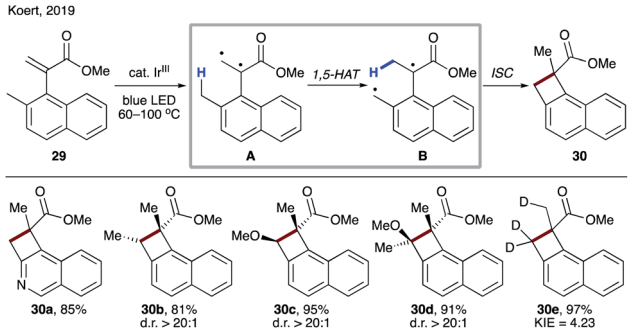

Scheme 9 Synthesis of cyclobutanes **30** *via* EnT-induced 1,5-HAT to a 1,2-biradical.

napthyl) acrylates **29**.[29] 1,2-Biradical **A**, formed by energy transfer (EnT) from a photoexcited iridium catalyst, underwent 1,5-HAT to produce intermediate **B**. In contrast to the above cases, instead of the formation of *o*-xylylene, cyclobutane **30** is furnished after ISC/recombination of radicals. Thus, this transformation represents a carbon analogue of Norrish–Yang reaction. The reaction performed with a deuterium-labelled substrate provided evidence for 1,5-HAT, as well as it being the rate-determining step (**30e**) (Scheme 9).

In 2014, Liu, Tan, and co-workers reported enantioselective C–H alkoxylation involving a 1,5-HAT process (Scheme 10a).[30a] The trifluoromethyl radical, formed by single electron reduction of Togni's reagent by a copper(I) catalyst, undergoes radical addition to substrate **31**. A subsequent 1,5-HAT occurs to form more stabilized α-amido radical **B**, followed by a single electron oxidation to produce imine intermediate **C**. Finally, the nucleophilic attack of alcohol in the presence of chiral phosphoric acid (CPA) furnishes enantioenriched product **32**. The authors also demonstrated the feasibility of HAT with an aliphatic amide (**32d**). Later, a related transformation that also relied on 1,5-HAT was disclosed (Scheme 10a).[30b] In this case, a catalytic amount of 1,2-bis(diphenylphosphino)benzene (dppBz) serves as a single electron reductant and generates the trifluoromethyl radical with Togni II reagent under thermal conditions. Similarly, radical addition to **33** leads to the more stabilized radical **B**. Electron transfer to another equivalent of Togni II reagent, followed by a proton loss leads to, in contrast to an imine in the first report, enamide **C**, which is susceptible to another radical addition. Single electron oxidation followed by proton loss delivers the reaction product **34** and regenerates the phosphine catalyst, respectively. A one-pot procedure was also developed for the synthesis of various 5-(trifluoromethyl)oxazoles such as **35** (Scheme 10b).

A reaction mode where 1,5-HAT is induced by radical addition to a tethered double bond has proven to be efficient and general. Based on this strategy, transformations targeting weak C–H bonds, including benzylic (Scheme 11a),[31] α-carbonyl (Scheme 11b),[32] α-hydroxyl (Scheme 11c),[31a,33] and formyl (Scheme 11d),[34] have been developed. Notably, these substrates are also amenable to entropically less favored 1,6- and 1,7-HAT due to the presence of radical-stabilizing groups.

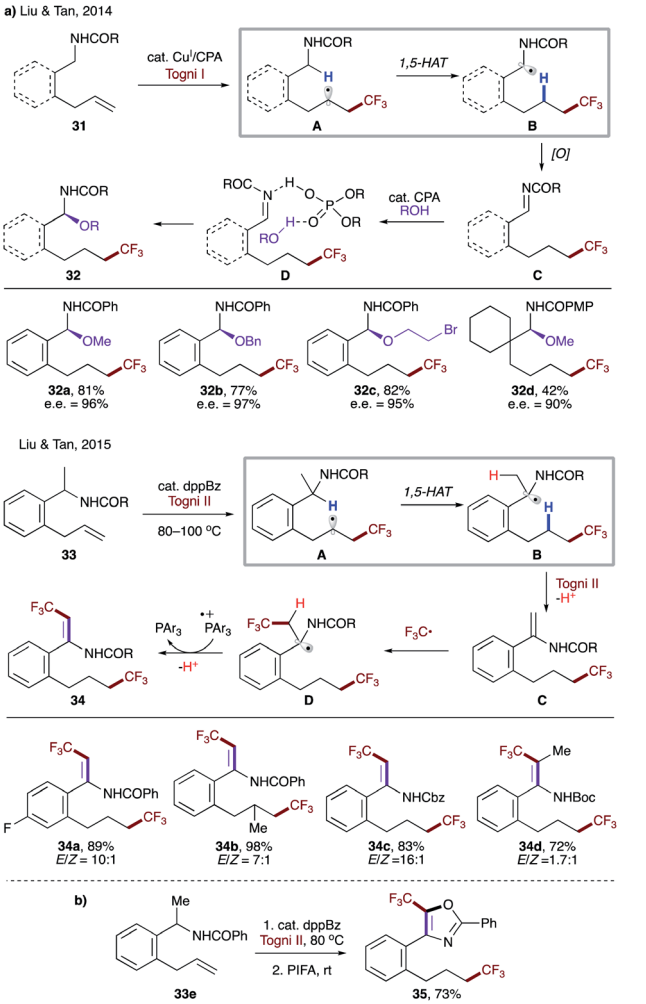

Scheme 10 (a) Radical addition-triggered 1,5-HAT. (b) One-pot synthesis of 5-(trifluoromethyl)oxazole **35**.

Very recently, Wang and co-workers reported iron-catalyzed remote functionalization that operates in a similar fashion.[35] Remarkably, the catalytic system could be applied not only to activated systems, but also to unactivated ones (Scheme 12). Notably, substrate bearing secondary C–H sites could also be employed (**56c**).

1,7-HAT. In 1997, Fuchs' group disclosed examples of 1,7-HAT to C(sp^3)-centered radicals (Scheme 13).[36] Under classical free radical conditions, (bromomethyl)silyl species **57** is converted to the corresponding silylmethyl radical **A**, which then engages in a 1,7-HAT process leading to the translocated radical **B**. A facile elimination of the arylsulfonyl radical then affords olefin product **58**. Both secondary (**58a–c**) and primary (**58d**) C–H sites were amenable to HAT giving good yields of alkenes, except for **58c** due to competing abstraction of benzylic hydrogens. The uncommon 8-membered transition state for this HAT transformation can be attributed to the increased tether length possessing sulfur and silicon atoms. Mechanistic studies ruled out the possibility of an intermolecular HAT event.

In 2013, Beau, Urban and co-workers reported selective mono-debenzylation of benzyl-protected carbohydrate

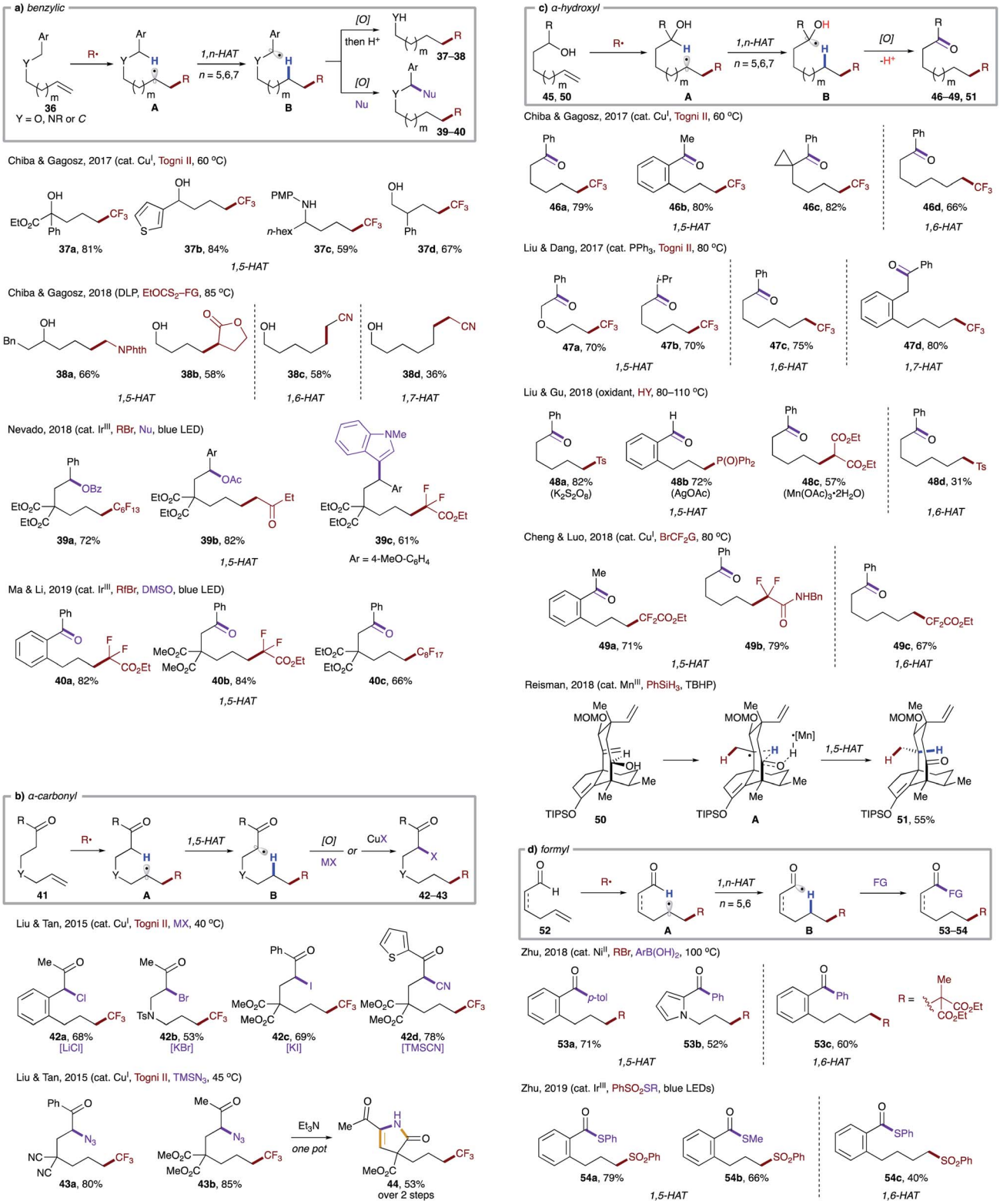

Scheme 11 Intramolecular HAT from activated C–H bonds initiated by radical addition to a tethered olefin. (a) Benzylic C–H. (b) α-Carbonyl C–H. (c) α-Hydroxyl C–H. (d) Formyl C–H.

templates **59** that involved a key 1,7-HAT step triggered by a silylmethyl radical (Scheme 14a).[37] The substrates were readily converted to the corresponding xanthate methylsilyl ethers **60** *via* a sequential silylation and substitution by xanthate. Thermal decomposition of dilauroyl peroxide (DLP) initiates the process to produce electrophilic silylmethyl radical

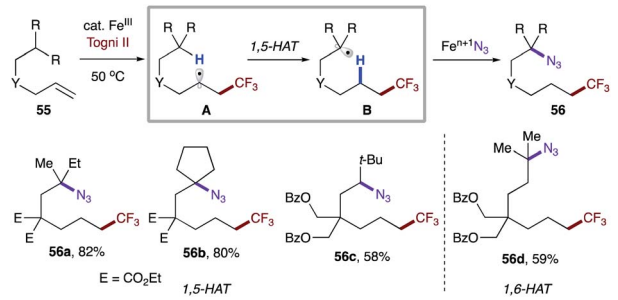

Scheme 12 Intramolecular HAT from unactivated C–H bonds.

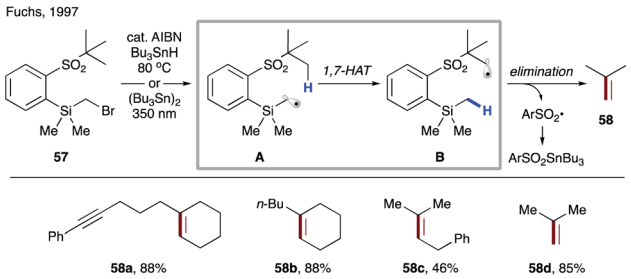

Scheme 13 Formation of an alkene *via* 1,7-HAT/β-elimination of **57**.

intermediate **A**, which undergoes 1,7-HAT to furnish benzylic radical **B**. Oxidation of the latter by DLP generates a stable benzylic cation, which is trapped in the form of acyl acetal **C**. A subsequent hydrolysis and desilylation delivers the reaction product, diol **61**. In the case of β anomers such as **60a**, an alternative path could be operational, which involves a successive 1,5-HAT from anomeric C–H and then benzylic C–H sites (Scheme 13b). However, the authors discounted this possibility as α anomer **60b**, which does not possess suitable hydrogen at the anomeric site, reacted smoothly to give **61b** with similar efficiency (Scheme 13c).

Later in 2015, the group of Zeng, Ren and Wu utilized the 1,7-HAT process in the construction of an isocopalane skeleton (Scheme 15).[38] Radical precursor **63** was readily prepared from naturally abundant andrographolide **62**. Upon heating, **63** undergoes homolytic cleavage of the S–Cl bond and SO_2 extrusion leading to primary alkyl radical **A**. 1,7-HAT then follows, resulting in the more stable α-acyloxy- or α-alkoxy radical **B**. Finally, fragmentation of **B** affords the reaction product, aldehyde **64**. Deuterium labelling studies confirmed the migration of the hydrogen atom, thus ruling out a sequential 1,5-HAT (*vide supra*). Furthermore, catalytic amounts of benzoyl peroxide accelerated the reaction while TEMPO shut down the reaction, suggesting a radical pathway for this transformation. Several protecting groups R were examined, which led to moderate to good yields (**64a–d**), with the exception of the benzoylated substrate (**64e**). Interestingly, methyl ether was a viable substrate (**64f**).

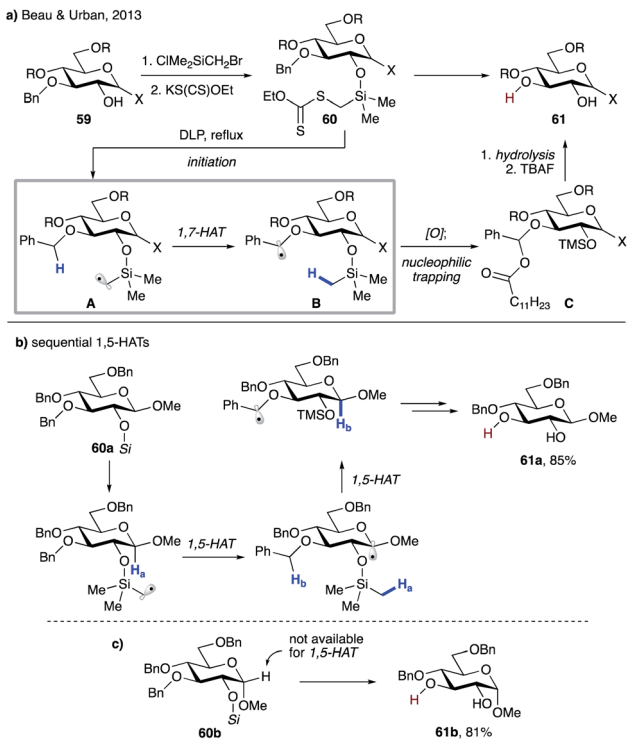

Scheme 14 (a) Selective mono-debenzylation of **59**. (b) Plausible mechanism for sequential 1,5-HATs leading to the same product. (c) Validation of 1,7-HAT based on efficient debenzylation of **60b**.

Intramolecular HAT at competing sites

In 2017, Gevorgyan and co-workers demonstrated the ability of hybrid alkyl palladium-radical species to undergo selective intramolecular HAT at unactivated C(sp^3)–H sites, featuring an easily installable/removable silicon-based auxiliary (Scheme 16).[39] Substrate **65**, readily accessible *via* routine silyl protection of the corresponding alcohol, engages in a single electron transfer (SET) with a photoexcited Pd(0) catalyst to form hybrid radical **A**, which undergoes rate-limiting site-selective 1,*n*-HAT

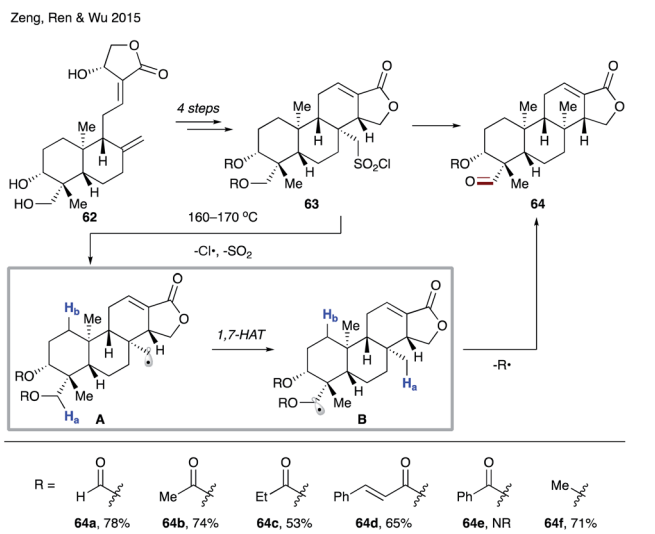

Scheme 15 Construction of isocopalane framework **64** involving 1,7-HAT.

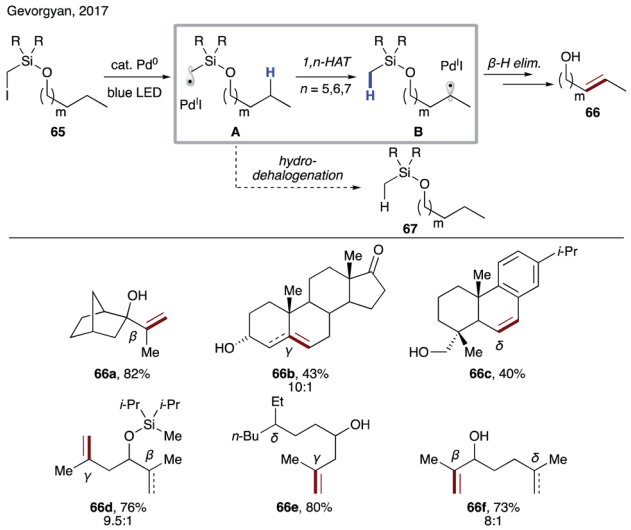

Scheme 16 Remote desaturation of aliphatic alcohols *via* selective 1,*n*-HAT enabled by an iodomethylsilyl auxiliary.

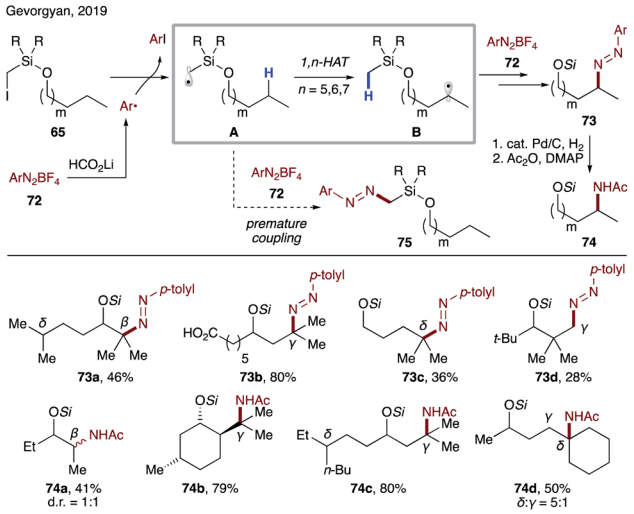

Scheme 18 Transition metal- and light-free remote amination of aliphatic alcohols.

to produce translocated radical **B**. The latter may either recombine with Pd(I) followed by β-hydride elimination, or undergo direct HAT with Pd(I) to furnish remote desaturation product **66** after desilylation with TBAF. A side hydrodehalogenation process, which would produce reduced product **67**, was suppressed under optimized conditions. This protocol allows for activation of both secondary and tertiary C(sp^3)–H bonds at β-, γ-, and δ sites (**66a–c**). Remarkably, a high level of site-selectivity was maintained even with substrates bearing competitive sites with similar BDEs (**66d–f**). Kinetic studies suggested the selectivity preference to be 1,6-HAT (γ) > 1,5-HAT (β) > 1,7-HAT (δ). The preference of 1,6-HAT over the more common 1,5-HAT can be attributed to the increased tether length and flexibility of the tether possessing silicon atom.[40] This method represents the first practical catalytic desaturation of aliphatic alcohols under mild, auxiliary-enabled, visible light-induced conditions.

Photoexcited palladium catalysis has been developed for alkyl Heck reaction and C–H activation,[41] which had not been utilized synergistically to achieve more complex transformations. Very recently, Gevorgyan's group disclosed site-selective radical relay Heck reaction of aliphatic alcohol derivatives **65** with various alkenes **68** to achieve alkenylation at remote unactivated C(sp^3)–H sites (Scheme 17).[42] Potential side

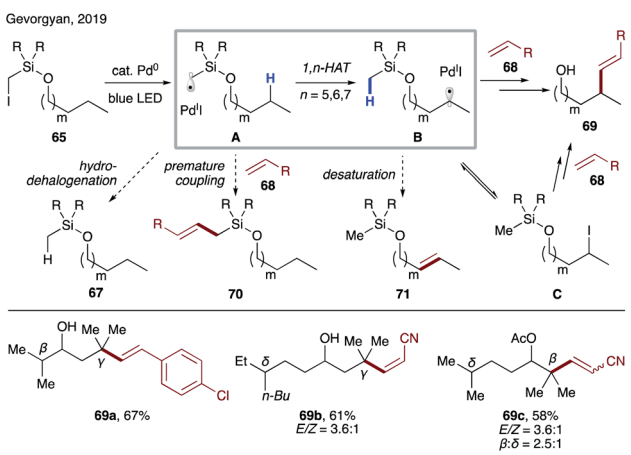

Scheme 17 Radical relay Heck reaction of aliphatic alcohols.

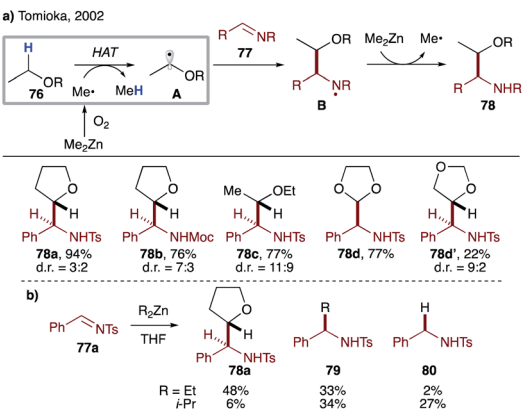

Scheme 19 (a) Intermolecular HAT from **76** to the methyl radical. (b) Superiority of the methyl radical *vs.* ethyl- and isopropyl radicals.

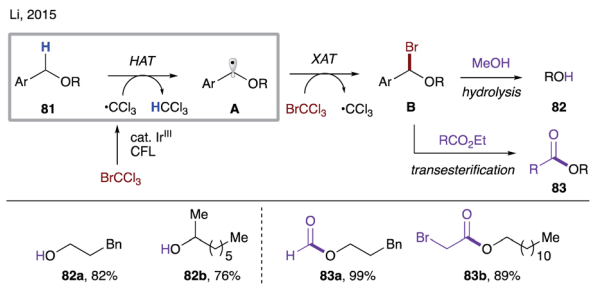

Scheme 20 Employment of the trichloromethyl radical in intermolecular HAT.

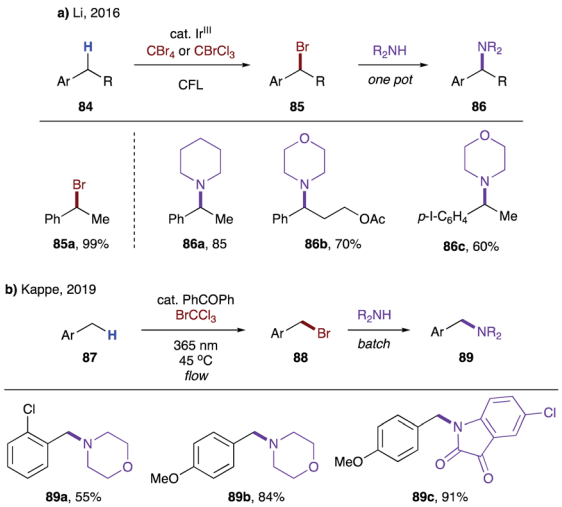

Scheme 21 Benzylic C–H bromination *en route* to benzyl amines *via* intermolecular HAT. (a) Secondary benzylic C–H. (b) Primary benzylic C–H.

reactions, such as premature Heck reaction (**70**) and desaturation (**71**), were suppressed under optimized conditions. Interestingly, iodide **C** was observed over the course of reaction, which was shown to produce alkenol **69** under reaction conditions, thus suggesting its intermediacy in this transformation. As in the previous case (Scheme 16),[39] this reaction exhibits the same site-selectivity: γ > β > δ.

In continuation of employing silicon-based tethers for remote transformations, Gevorgyan's group reported a transition metal- and light-free directed amination of **65** (Scheme 18).[16] This method represents the first general approach for selective amination of inert C(sp^3)–H bonds at β-, δ-, and γ sites. In the presence of lithium formate, readily available aryl diazonium salt **72** is reduced to generate an aryl radical, which abstracts an iodine atom from the substrate. The resultant silyl methyl radical **A** is electrophilic and thus not predisposed to premature coupling with **72**. As such, the desired 1,*n*-HAT occurs, leading to a transposed nucleophilic radical **B**, which undergoes facile radical addition to **72** to furnish diazenylation product **73**. It is noteworthy that the primary C–H site is also reactive under the conditions of this method (**73d**). In addition, protected amino alcohols **74** can be obtained in reasonable yields *via* a one-pot three-step protocol.

Intermolecular HAT

Efficient transformations involving intermolecular HAT mediated by sp^3-hybridized C-centered radicals are rare due to a smaller thermodynamic driving force, as compared to those mediated by C(sp^2)-, N- or O-centered radicals. In 2002, Tomioka's group utilized the instability of the methyl radical to achieve intermolecular radical addition of ethers to aldimines (Scheme 19a).[43] Dimethylzinc and oxygen initiate the reaction by producing a methyl radical, which abstracts activated α-hydrogen from ethereal solvent **76** to generate nucleophilic radical **A**. The latter then adds to aldimine **77** to give aminyl radical **B**, which is reduced by dimethylzinc to furnish product **78** after aqueous workup. Meanwhile, the methyl radical is regenerated to close the radical chain cycle. Both cyclic and linear ethers are suitable substrates, albeit with moderate diastereoselectivity in most cases. Employment of diethylzinc and diisopropylzinc led to a drastic decrease in product yield due to significant formation of alkyl adduct **79** and/or reduction product **80**, highlighting the pivotal role of methyl radical in efficient intermolecular HAT (Scheme 19b). Direct HAT between **76** and N-centered radical **B** is unlikely, as the reaction requires a super-stoichiometric amount of zinc reagent. Later in 2003, the same group developed chemoselective addition of the THF radical to aldehydes under Et_3B/air conditions.[44] This initiator-dependence was also applied to three-component reaction of aldehyde, amine and THF.

Given the relatively small thermodynamic driving force for the HAT step to the C-based radicals, the polarity match becomes an increasingly important factor. In 2015, the Li group reported visible light-promoted transesterification and debenzylation reactions of alkyl benzyl ethers **81** (Scheme 20).[45a] The trichloromethyl radical is first generated *via* a single electron reduction of bromotrichloromethane by a photoexcited iridium catalyst.[46] A polarity-matched intermolecular HAT between this electrophilic radical and the electron-rich C–H bond in **81** occurs, resulting in nucleophilic radical **A**. A subsequent halogen atom transfer (XAT) produces α-bromoether **B** and a trichloromethyl radical, thereby propagating the radical chain process. Intermediate **B** can either be hydrolysed in methanol in a one-pot two-step manner to the debenzylation products **82** or undergo *in situ* transesterification to afford esters **83**.

Later, Li's group showed that substrates possessing secondary benzylic C–H bonds (**84**) are also competent for analogous bromination, thus affording benzyl bromides **85** in good to excellent yields (Scheme 21a).[45b] In addition, a one-pot synthesis of benzyl amines **86** was developed, albeit a huge excess of amine was required to achieve good yields. In 2019, Kappe and co-workers disclosed the same process for toluene derivatives **87** under a continuous flow reaction setup using benzophenone as a photocatalyst (Scheme 21b).[45c] Moderate yields of benzylamines **89** were obtained when **87** was susceptible to dibromination (**89a**).

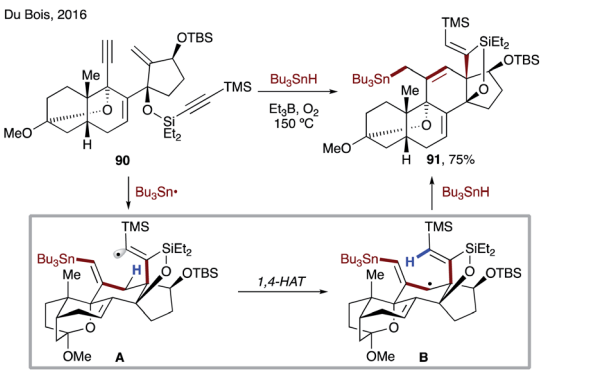

Scheme 22 Synthesis of the steroidal core of batrachotoxin *via* 1,4-HAT of a vinyl radical.

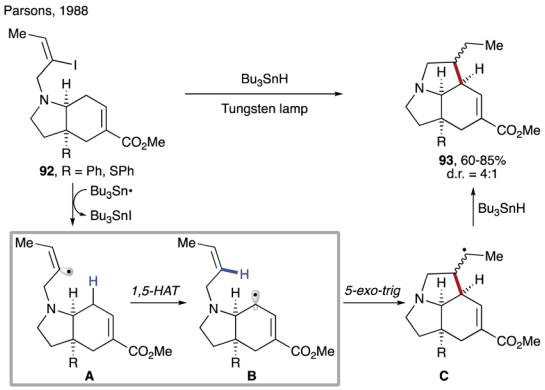

Scheme 23 1,5-HAT triggered by a vinyl radical in the synthesis of a pyrrolizidine ring system.

HAT involving vinyl radicals

A larger BDE difference between olefinic C–H (~110 kcal mol^{-1}) and aliphatic C–H (~96–100 kcal mol^{-1}) bonds makes the 1,*n*-HAT process more efficient compared to that by an alkyl radical.[47] According to studies by Gilbert and co-workers, the rate of 1,5-HAT at the activated C–H site by a vinyl radical is more than 10^5 s^{-1}.[48] After the HAT process, usually the alkene moiety serves as a radical acceptor for the translocated radical, leading to the formation of cyclopentane or cyclohexane derivatives.[49] In general, a vinyl radical is generated by halogen abstraction/single electron reduction of the corresponding vinyl halides or *via* radical addition to alkynes.[50] The second approach is more attractive from a practical standpoint, since the first protocol requires synthesis of vinyl halides. However, despite being exothermic in nature, the intermolecular radical addition to an alkyne is a relatively slow process. The feasibility of HAT by vinyl radicals was first reported in 1967 by Heiba and Dessau in the novel radical cascade involving addition of $^{\bullet}CCl_3$ across a triple bond that triggered 1,5-HAT.[50b] However, it was not until 1988 when the first systematic studies on 1,5-HAT of vinyl radicals were reported by Parsons.[9b]

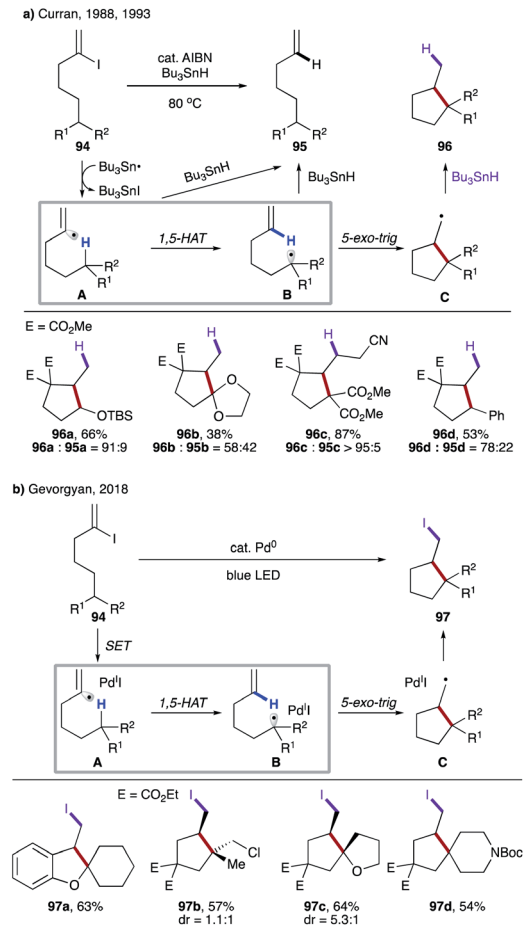

Scheme 24 (a) Free radical translocation *via* 1,5-HAT. (b) 1,5-HAT of the hybrid vinyl palladium radical intermediate.

Intramolecular HAT

1,4-HAT. 1,4-HAT of vinyl radicals has rarely been observed, typically in sterically constrained substrates, usually as a side reaction. First 1,4-HAT was implemented by Malacria and co-workers in the synthesis of enantiomerically pure 1,2,3-triols.[51]

In 2016, Du Bois and co-workers achieved concise asymmetric synthesis of the natural (−) and non-natural (+) antipodes of batrachotoxin, as well as both enantiomers of a C-20 benzoate-modified derivative (Scheme 22).[52] The key radical cascade sequence involving 1,4-HAT of a vinyl radical formed *in situ* is highly efficient and selective. The process commences with addition of a tributyl tin radical at the terminal alkyne of **90**, followed by sequential 6-*endo-trig*/5-*exo-dig* cyclizations to produce reactive intermediate **A**. This electrophilic radical then undergoes 1,4-HAT to form stabilized nucleophilic allylic radical species **B**, which is quenched by Bu_3SnH to deliver **91** in 75% yield.

1,5-HAT. In 1988, Parsons' group first demonstrated that vinyl radicals could undergo translocation to alkyl sites *via* intramolecular HAT (Scheme 23).[9b] In the presence of Bu_3SnH and tungsten lamp irradiation, the vinyl radical **A** generated from vinyl iodide **92** undergoes 1,5-HAT to afford translocated allylic radical **B**. 5-*Exo-trig* cyclization of the latter, followed by reduction efficiently leads to the desired pyrrolizidine ring system **93** as a mixture of epimers.

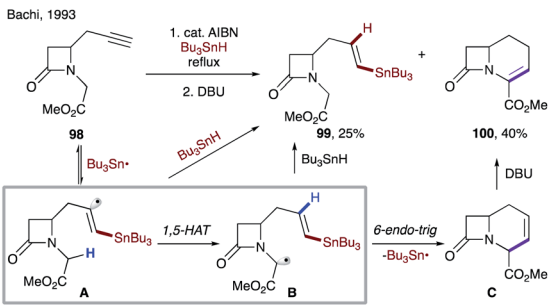

Scheme 25 1,5-HAT of a vinyl radical in the synthesis of bicyclic β-lactam.

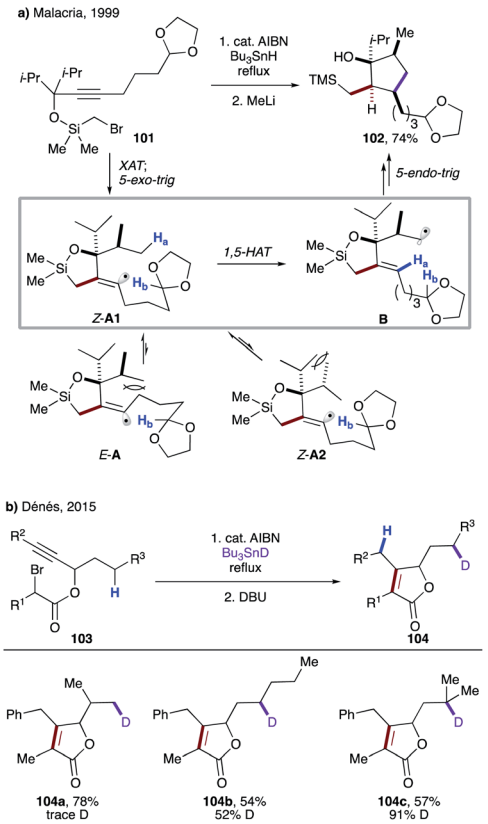

Scheme 26 (a) Diastereoselective 1,5-HAT event triggered by 5-*exo-dig* cyclization, followed by 5-*endo-dig* cyclization. (b) 5-*Exo-dig* cyclization followed by "invisible" 1,5-HAT.

In their seminal work, Curran's group reported translocation of vinyl radicals *via* 1,5-HAT (Scheme 24a).[9a] Realising that C–H bonds, the most attractive and simplest 'radical precursor', could not be activated *via* intermolecular HAT by a tin radical due to its significantly endothermic nature, they utilized Bu_3SnH as an atom transfer agent to access vinyl radical **A** from **94**. Efficient 1,5-HAT occurs to form translocated alkyl radical **B**, which is cyclized to produce cyclopentane derivatives **96** after reduction. A premature reduction of the vinyl radical *via* intermolecular HAT leads to the acyclic alkene byproduct **95**. In 1993, Curran's group disclosed the substituent effect on these types of 1,5-HAT transformations.[53] Although a few exceptions exist, the authors found a correlation between the rate of 1,5-HAT and the BDE of the C(sp^3)–H bond. They also found that the overall geometry of the moiety undergoing HAT was likely to have a greater impact than the particular substituent at the target C–H site.

In 2018, Gevorgyan's group reported photoinduced palladium-catalyzed non-chain atom transfer radical cyclization (ATRC) at remote unactivated aliphatic C–H sites with similar types of substrates (Scheme 24b).[54] The hybrid vinyl palladium-radical **A** undergoes a 1,5-HAT process to generate the translocated radical **B**, which upon 5-*exo-trig* cyclization leads to the intermediate **C**. Finally, iodine atom transfer from the putative Pd(I)I affords iodomethyl carbo- and heterocyclic motifs **97**, thus contrasting with the reductive transformation by Curran.

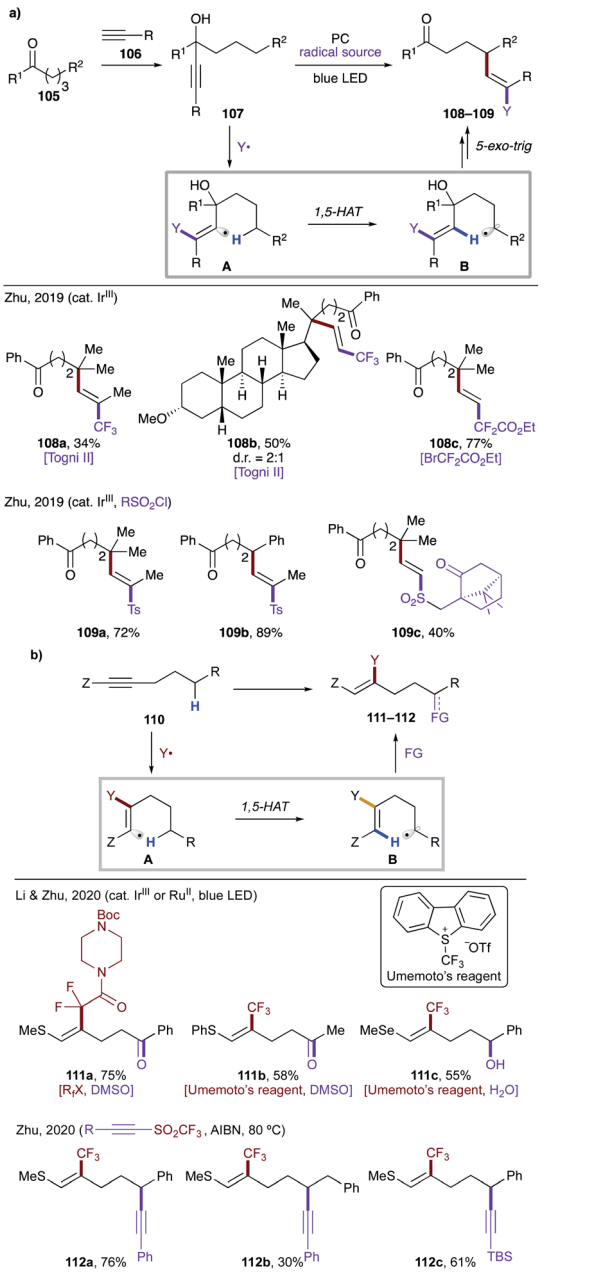

Scheme 27 (a) Regioselective vinylation *via* 1,5-HAT, triggered by radical addition to an alkyne. (b) Remote C–H functionalizations of an alkyne *via* 1,5-HAT of a vinyl radical formed by β-radical addition.

Notably, no formation of Heck-type products *via* β-hydrogen elimination of the radical intermediate **C** was observed.

As discussed above, the alternative way to form vinyl radicals involves addition of radicals to alkynes. In 1967, Heiba and Dessau observed 1,5-HAT of a vinyl radical during addition of polyhalomethanes to terminal alkynes.[55] In 1993, Bachi and co-workers reported the formation of vinyl radical **A** *via* addition of the tributyltin radical to an alkyne moiety of **98.** A subsequent 1,5-HAT, followed by 6-*endo-trig* cyclization and β-tin elimination produces β-lactam **C** (Scheme 25).[56] Upon DBU-catalyzed isomerization of the double bond, methyl 1-oxahomoceph-4-

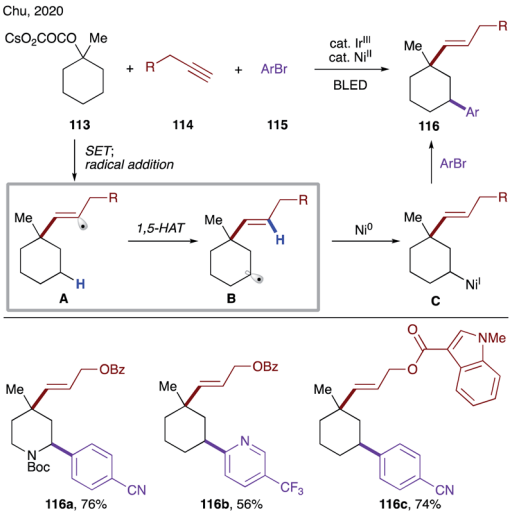

Scheme 28 Photoredox/nickel dual-catalyzed radical cascade involving 1,5-HAT of vinyl radicals.

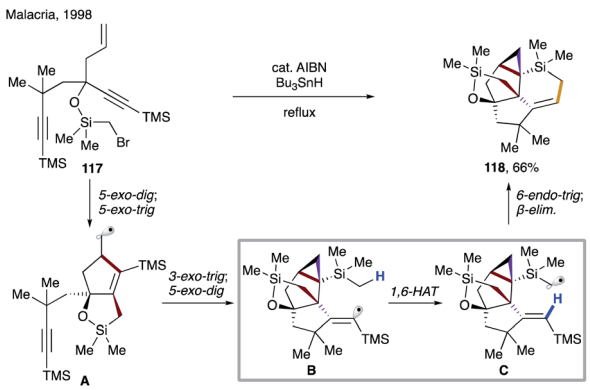

Scheme 29 Highly diastereoselective 1,6-HAT in the synthesis of triquinane derivatives.

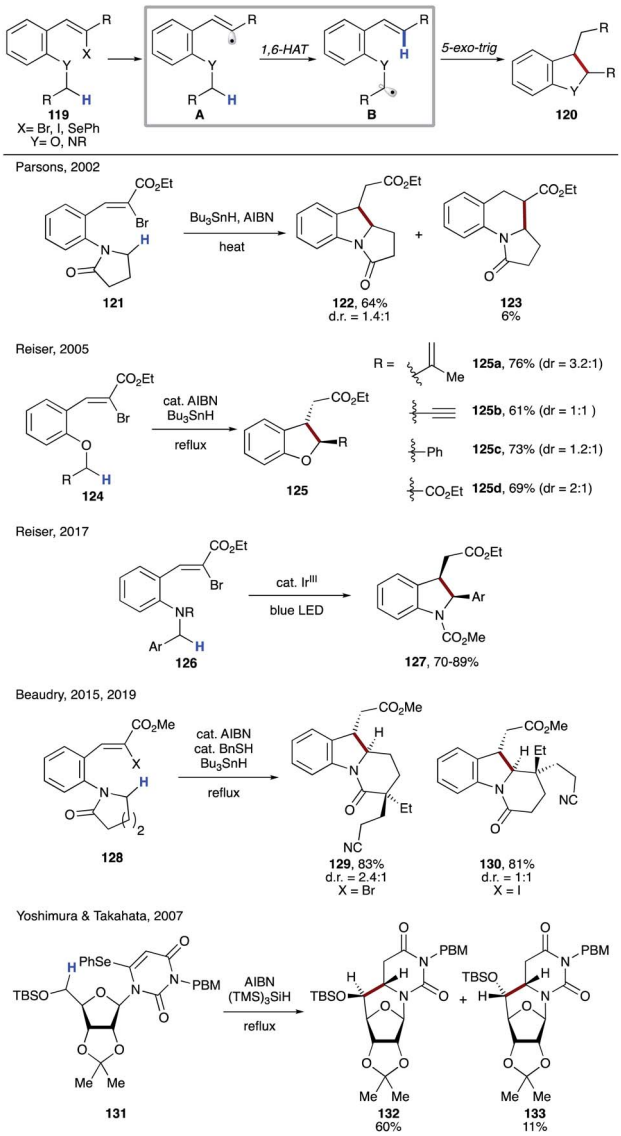

Scheme 30 Cascade radical reactions of vinyl radicals involving 1,6-HAT at C(sp^3)–H sites α to the heteroatom.

em-5-carboxylate **100** was obtained in 40% yield, along with 25% of reduction byproduct **99**.

Few years later, Malacria's group reported an efficient radical cascade reaction for diastereoselective synthesis of highly functionalized cyclopentanes (Scheme 26a).[57] In this transformation, substrate **101** forms an α-silyl radical upon XAT, which then cyclizes to give vinyl radical species **A**. 1,3-Allylic interaction in *E*-**A** and eclipsed interaction between methyl and isopropyl groups in *Z*-**A2** render them less favourable conformers than *Z*-**A1**. The latter undergoes highly regioselective 1,5-HAT at the unactivated C(sp^3)–H site, leading to primary alkyl radical intermediate **B**. A following rarely observed 5-*endo-trig* cyclization constructs the cyclopentane moiety. Finally, the cleavage of the siloxy ring with MeLi affords product **102** in impressive 74% overall yield.

Recently, Dénés' group disclosed the involvement of 1,5-HAT in a similar type of reaction sequence during the synthesis of polysubstituted γ-butenolides (Scheme 26b).[58] The deuterium labelling experiments revealed an "invisible" 1,5-HAT to the formed vinyl radical from the aliphatic side chain. Expectedly, due to the greater stability of the tertiary radical, the higher deuterium incorporation was observed in **104c**.

In 2019, Zhu and co-workers reported mild, photocatalytic methods for activation of δ C(sp^3)–H bonds *via* formation of vinyl radicals (Scheme 27a).[59] In both cases, the authors synthesized the tertiary propargyl alcohol derivatives **107** *via* addition of acetylide **106** at ketone **105**. Under the reaction conditions, the excited photocatalyst undergoes SET to generate electrophilic radical Y˙, which adds to an alkyne to trigger a 1,5-HAT event. The translocated radical species **B** undergoes a sequence of 5-*exo-trig* cyclization, β-elimination and oxidation by a photocatalyst to afford the final product **108–109**. Using this protocol, valuable, complex fluoroalkylated alkenes **108a–c**,[59a] and sulfonylvinylation products **109a–c** (ref. 59b) were easily accessed.

Recently, Li, Zhu and co-workers reported remote functionalization of heteroalkyne **110** *via* HAT of a vinyl radical formed by β-radical addition (Scheme 27b).[60] The method involves addition of a perfluoroalkyl radical to an alkyne to generate vinyl radical **A**, which undergoes 1,5-HAT to produce nucleophilic alkyl or benzyl radicals **B**. In the first scenario, the translocated radical **B** is oxidized selectively to ketone or alcohol **111a–c**, while in the second case, the radical **B** is trapped by an electrophilic alkyne to afford remote alkynylation products **112a–c**.

Very recently, Chu's group developed photoredox/nickel dual-catalyzed conditions for sequential deoxygenative vinylation/C–H arylation of tertiary oxalates (Scheme 28).[61] This multicomponent cascade is initiated by a single electron oxidation of oxalate **113** by a photoexcited iridium catalyst, which results in decarboxylation, followed by addition of the formed tertiary alkyl radical to alkyne **114** to form vinyl radical **A**. The succeeding 1,5-HAT affords a translocated secondary alkyl radical **B**, which is captured by Ni(0) to form alkyl Ni(I) species **C**. The reaction product **116** is obtained upon nickel-mediated cross-coupling with an aryl halide.

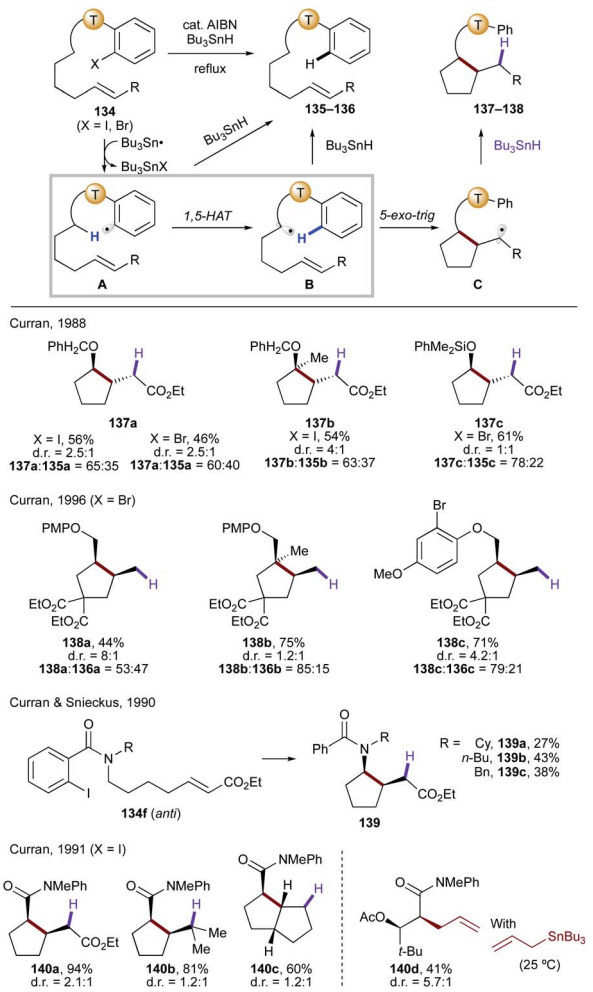

Scheme 31 Translocation of radicals from C(sp^2) to C(sp^3) sites *via* 1,5-HAT, followed by cyclization to afford cyclopentane derivatives.

1,6-HAT. In 1998, Malacria and co-workers demonstrated an impressive cascade polycyclization toward efficient and highly diastereoselective assembly of a triquinane core that features five radical cyclizations and one 1,6-HAT step (Scheme 29).[62] In the presence of AIBN and Bu_3SnH, formation of the silyl methyl radical triggers the radical cascade, delivering **A** *via* successive 5-*exo-dig* and 5-*exo-trig* cyclization, followed by a rare 3-*exo-trig* and 5-*exo-dig* cyclizations to generate α-silyl vinyl radical **B**. The latter undergoes 1,6-HAT at the silylmethyl C(sp^3)–H site to form a primary silylmethyl radical, which upon cyclization followed by β-silyl elimination affords the product **118** in 66% yield.

Several examples of radical cascade reactions showcased the formation of electrophilic vinyl radical **A** generated from **119**, which undergoes 1,6-HAT to form nucleophilic α-heteroatomic radical **B**. A subsequent 5-*exo-trig* cyclization, followed by reduction of the forming alkyl radical affords the cyclic product **120** (Scheme 30). In 2002, Parsons and co-workers utilized this strategy to synthesize **122**, the precursor of mitomycin ring systems.[63] Few years later, Reiser's group reported the synthesis of 2,3-disubstituted dihydrobenzofurans **125a–d** involving a similar type of 1,6-HAT process.[64] In 2017, the same group employed photoredox catalysis to synthesize 2,3-disubstituted indolines **127** using a similar strategy.[65] Beaudry and co-workers also utilized this 1,6-radical translocation strategy to construct the central indoline core of several natural products (**129**, **130**).[66] In 2007, Yoshimura, Takahata, and co-workers reported the synthesis of 6,5′-C-cyclouridines **132** and **133**, in which the tris(trimethylsilyl)silyl (supersilyl) radical initiates the process by selenium abstraction in **131**.[67]

HAT involving aryl radicals

Aryl radicals are extremely reactive species. Similarly to HAT to vinyl radicals, HAT to aryl radicals from aliphatic C–H sites is energetically favourable due to the high BDE difference between aryl C–H bonds (Ph–H, BDE = 112 kcal mol^{-1}) and aliphatic C–H bonds (BDE ∼ 96–100 kcal mol^{-1}).[47] In 1954, Hey and co-workers recognized intramolecular 1,5-HAT during the decomposition of *o*-(dimethylaminocarbonyl)aryl or (*N*-aryl-*N*-methylaminocarbonyl)aryl diazonium salts.[8] Later, Cohen and co-workers also showed that aryl radicals could undergo 1,5-HAT during copper-catalyzed decomposition of diazonium salts, which was supported by extensive mechanistic studies.[68] The

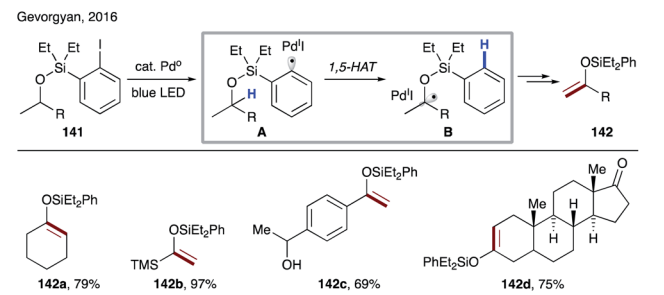

Scheme 32 HAT event of hybrid Pd-radical species.

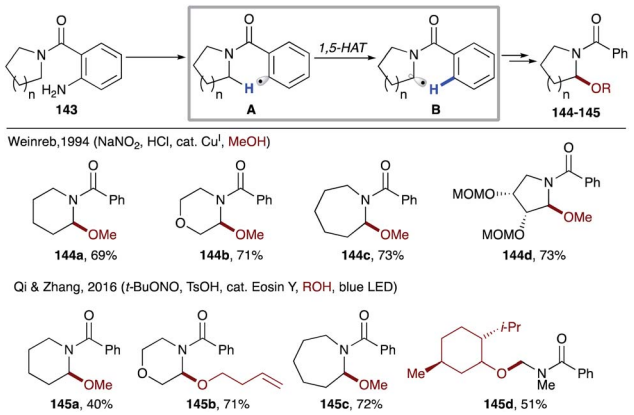

Scheme 33 Oxidation of amides *via* 1,5-HAT.

deuterium labelling experiments suggested that the rate of 1,5-HAT is much faster than the rotation around the amide C–N bond but slower than that of the methyl C(sp^3)–N bond, presumably due to the partial double bond character of the former. In 1978, Pines and co-workers reported the intramolecular HAT process of aryl radicals generated from different *ortho*-substituted aryl diazonium salts. Furthermore, intramolecular 1,5-, 1,6-, and 1,7-HATs were observed during copper-catalyzed decomposition of *o*-di-*n*-propylaminosulfonylbenzenediazonium salts.[69]

Intramolecular HAT

1,5-HAT. In their pioneering studies, Curran's group reported translocation of radicals from C(sp^2) to C(sp^3)–H sites *via* 1,5-HAT.[9a,70] Incorporated into a modified 'protecting group' of alcohols, an aryl radical serves as an HAT agent to produce a translocated alkyl radical (Scheme 31). The latter is trapped intramolecularly followed by reduction by tin hydride to deliver cyclopentane derivatives **137–140.** A premature reduction of radicals **A** or **B** *via* intermolecular HAT from Bu_3SnH could produce acyclic alkene byproducts **135–136.** As shown in their first report in 1988, introduction of a silicon-based tether led to an improvement of the product to side reduction byproduct ratio (**137c** *vs.* **135c**). Few years later, the same group introduced *o*-bromo-*p*-methoxyphenyl ethers as new radical translocating groups for β C–H bond activation (**138a–c**).[70] The deuterium labelling study showed that tertiary radicals were efficiently generated; however translocation of radicals to the secondary C–H sites was challenging due to a competitive 1,6-HAT process.

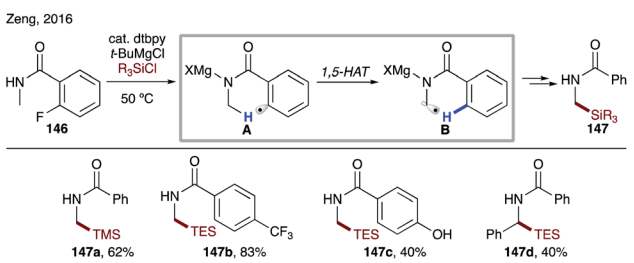

Scheme 34 Silylation of benzamides *via* 1,5-HAT.

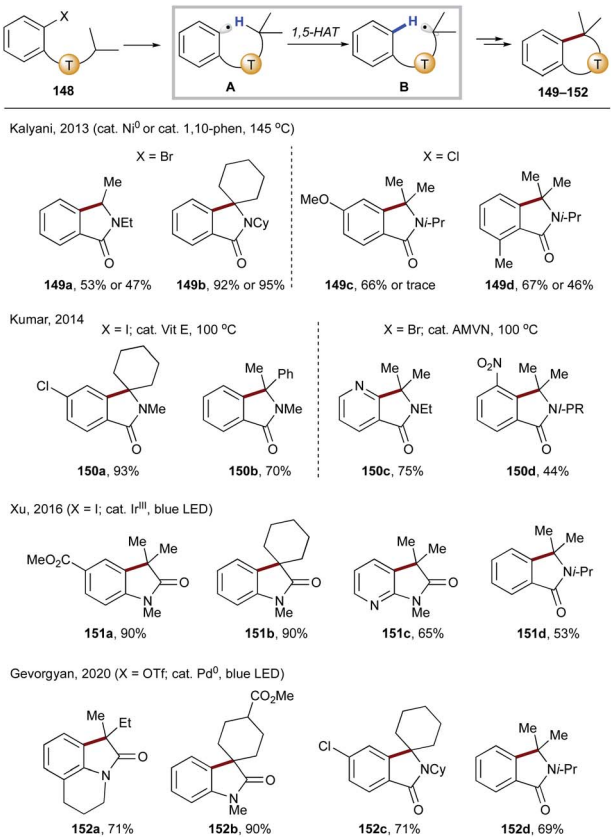

Scheme 35 Synthesis of fused systems *via* 1,5-HAT from the C(sp^3)–H to the C(sp^2) site followed by radical cyclization at the aromatic ring.

Introduction of *ortho* substituents (**138c**) improved the efficiency of the radical translocation process. Of note, in the absence of the double bond tether, extrusion of the stable benzylic radical occurs, leading to the corresponding aldehyde or ketone.[71]

Similarly, amides have also been utilized in the related process involving the 1,5-HAT step.[72] In the case of *o*-iodobenzamides,[72a,b] only the *anti*-rotamer of **134f** will lead to the desired cyclic product (**139a–c**). Thus, the reaction outcome is highly dependent on the R group as it affects the *anti*/*syn* ratio of the amide. On the other hand, employment of *o*-iodoanilides allows for the direct α C–H functionalization of carbonyl compounds without enol or enolate formation.[72c,d] The reaction is shown to be effective for intermolecular radical trapping of the translocated radical with deuterium or an allylic group (**140d**).

In 2016, Gevorgyan's group introduced a 1,5-HAT event of hybrid palladium-radical species (Scheme 32).[73] Aryl halides are well-known substrates in palladium catalysis, typically involved in a two-electron oxidative addition process. But in this case the authors have discovered that irradiation with blue light switched the reaction pathway leading to an SET process to generate hybrid palladium-radical species **A.** Due to the radical nature of this intermediate, it undergoes a 1,5-HAT process to generate translocated radical species **B**, which upon β-hydrogen loss delivers silyl enol ethers **142a–d.** In this light-induced

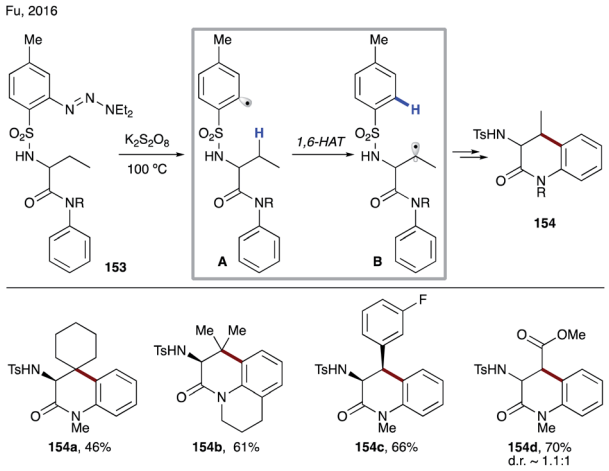

Scheme 36 Synthesis of cyclic anilides involving 1,6-HAT from the aliphatic C–H sites.

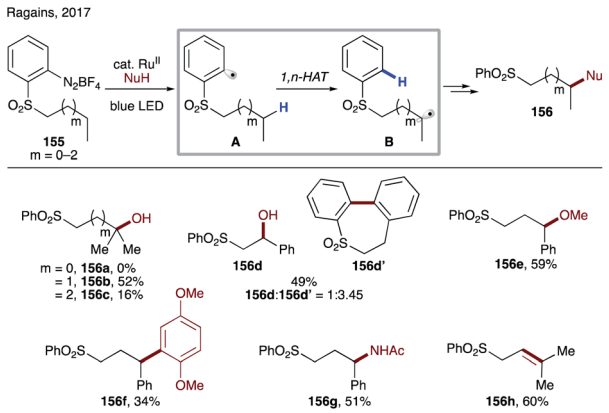

Scheme 37 1,6-HAT to the aryl ring of aryl sulfones from aliphatic C(sp^3)–H sites.

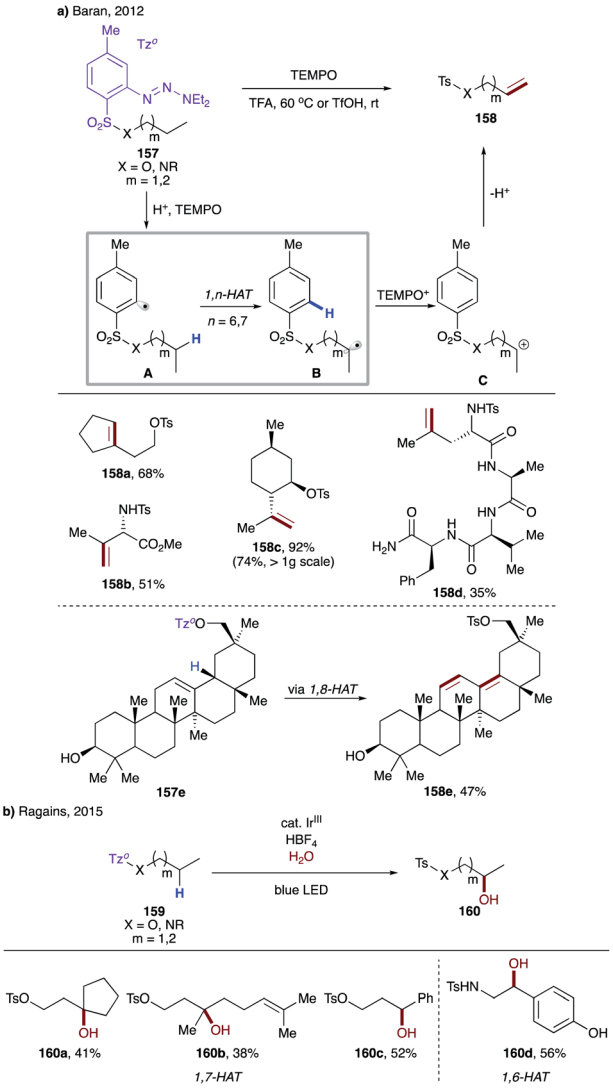

Scheme 38 (a) Guided desaturation of aliphatic alcohols and amines *via* intramolecular HAT. (b) Remote hydroxylation *via* intramolecular HAT.

protocol, palladium plays a double role by harvesting light and catalyzing the bond breaking/forming process. Notably, this mild method for dehydrogenation of silyl-protected alcohols to silyl enol ethers proceeds at room temperature without use of exogenous photosensitisers or oxidants.

In 1994, Weinreb's group utilized copper catalyzed diazotation of *o*-aminobenzamides **143** for oxidation of amides, which can also be translated to more complex systems like **144d**, used in the synthesis of antibiotic anisomycin (Scheme 33).[74] In this case, *in situ* diazotization of *o*-aminobenzamide **143**, followed by reduction *via* SET from a copper catalyst generates aryl radical **A**. 1,5-HAT of the latter affords nucleophilic radical **B**, which then *via* the copper-catalyzed radical-polar crossover process gets oxidized to an α-amino carbocation that is trapped by methanol to deliver products **144a–d**. Recently, Qi and Zhang's group reported photocatalytic, metal-free methods with similar types of substrates to achieve α-amino C(sp^3)–H functionalization.[75] Likewise, single electron reduction of the *in situ* formed diazonium salt by an excited Eosin Y photocatalyst leads to an aryl radical intermediate, which eventually affords α-alkoxybenzamides (**145a–d**) in moderate to good yields.

At the same time, Zeng and co-workers reported site-selective silylation of the α-amino C(sp^3)–H bond (Scheme 34).[76] The use of Grignard reagent enables generation of *N*-magnesiated aryl radical **A** from the corresponding fluoride **146**. This method represents the first example of α C–H silylation of amides.

It has been shown that in the absence of a tethered alkene as in the previous examples (Scheme 31), the translocated radical **B** can undergo radical addition to an arene, thus affording cyclization products **149–152** after rearomatization (Scheme 35). In 2013, Kalyani and co-workers reported the use of a nickel or phenanthroline catalyst for aryl chlorides and bromides to afford various isoindolin-1-ones **149a–d**.[77] Shortly after, Kumar's group developed metal-free conditions targeting bromides and iodides to deliver similar products (**150a–d**).[78] In 2016, Xu's group employed iridium photocatalysis to achieve

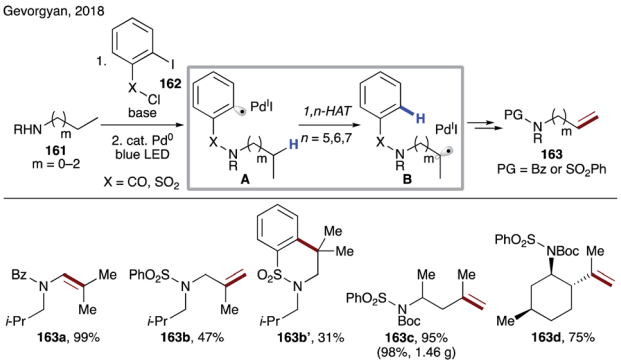

Scheme 39 Remote desaturation of aliphatic amines *via* HAT from the C(sp^3)–H site.

similar transformations (**148** → **151**) with iodides and its application to the formal synthesis of (±)-coerulescine and (±)-physovenine.[79] More recently, Gevorgyan and co-workers achieved the first photoinduced palladium-catalyzed C(sp^2)–O bond activation of an aryl triflate to form a hybrid aryl palladium-radical intermediate,[80] which underwent the same sequence of 1,5-HAT/radical cyclization to afford oxyindole and isoindolin-1-ones **152a–d**.

1,6-HAT. In 2016, Fu and co-workers reported transition metal-free, intramolecular, regioselective cross dehydrogenative coupling of aliphatic and aromatic C–H bonds (Scheme 36).[81] The authors used readily available aryl triazine **153** and a cheap oxidant, $K_2S_2O_8$, to generate under thermal conditions aryl radical **A**. The latter undergoes selective 1,6-HAT at the aliphatic C–H sites to afford translocated β-amino alkyl radical **B**, which cyclizes to from six membered cyclic anilides **154a–d**. Notably, phenyl alanine-derived substrates exhibit very high diastereoselectivity, leading to *cis* isomers (**154c**). In contrast, reactions of substrates containing aspartic acid derivatives led to a statistical mixture of diastereomers (**154d**).

Recently, Ragains' group developed photocatalytic reduction of *ortho*-diazoniaphenyl alkyl sulfones for remote C(sp^3)–H functionalization (Scheme 37).[82] First the photoexcited Ru-catalyst undergoes SET to diazonium salts **155**, followed by nitrogen loss leading to aryl radical **A**. This electrophilic aryl radical then undergoes intramolecular HAT at alkyl or benzylic C–H sites, preferably in a 1,6-fashion (**A** → **B**). The formed

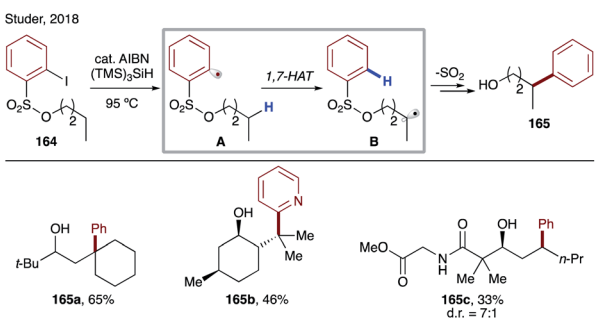

Scheme 40 Arylation of alcohols *via* 1,7-HAT, followed by aryl group migration.

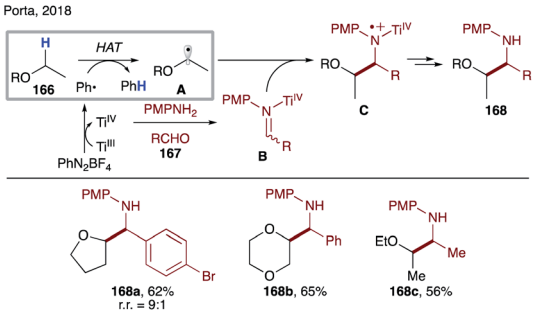

Scheme 41 Aminoalkylation of ethers *via* intermolecular HAT.

nucleophilic radical undergoes radical polar crossover *via* single electron oxidation by the photocatalyst or by the substrate *via* a chain process into a carbocation. A subsequent trapping of the latter with different nucleophiles affords remote hydroxylation (**156a–d**), etherification (**156e**), C–C bond formation (**156f**), amidation (**156g**), and desaturation (**156h**) products. In this protocol, the possibility of 1,5-HAT, as well as 1,7-HAT, was demonstrated, albeit with much lower efficiency.

1,7-HAT. In 2012, Baran's group established a dehydrogenation method for guided desaturation of unactivated C(sp^3)–H sites of alcohols and amines (Scheme 38a).[83] Under acidic conditions, aryl triazene **157** is *in situ* converted into a diazonium salt, which upon reductive decomposition leads to aryl radical **A**. The latter is capable of undergoing intramolecular HAT to form nucleophilic alkyl radical **B**, which is further oxidized to the corresponding carbocation *via* a radical polar crossover scenario (**B** → **C**) by $TEMPO^+$ formed at the early stages of the reaction. Loss of a proton affords remote desaturation products **158a–e**. For this sulfonyl tether, 1,7-HAT is more preferable; however, the presence of weaker β C–H bonds could lead to 1,6-HAT products (**158b**). It is also shown that even 1,8-HAT is possible at the activated allylic C–H site of **157e** to deliver diene **158e**.

In 2015, Ragains and co-workers uncovered remote hydroxylation of alcohols and amines with similar types of aryl sulfonyl tethers under photocatalytic conditions (Scheme 38b).[84] In this protocol, instead of TEMPO, a photocatalyst enables the single-electron redox process to afford after solvolysis the hydroxylation products **160a–d**. Expectedly, as in the above case, the aryl

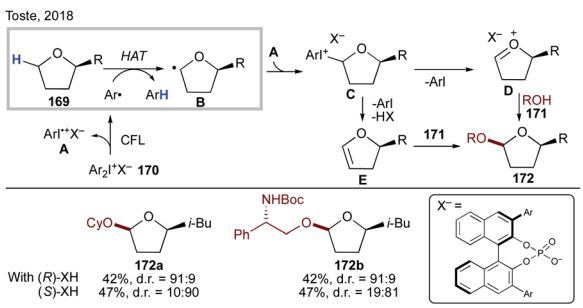

Scheme 42 Chiral diaryliodonium phosphate-mediated diastereoselective α-acetalization of cyclic ethers involving intermolecular HAT.

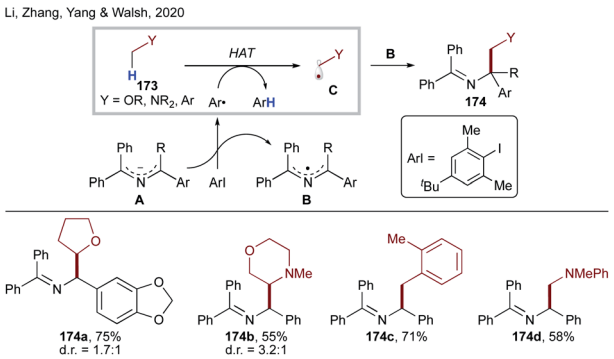

Scheme 43 Dehydrogenative cross-coupling *via* intermolecular HAT.

sulfonyl tether favours 1,7-HAT, unless a weaker benzylic C–H site is present to promote the 1,6-HAT event.

In 2018, Gevorgyan's group developed a mild photo-induced palladium-catalyzed protocol for proximal and remote desaturation of aliphatic amines (Scheme 39).[85] This method utilizes readily available 2-iodocarbonyl or 2-iodosulfonyl tethers (**162**) which can be routinely installed and do not require isolation. Under the reaction conditions, photoexcited palladium undergoes single electron transfer to aryl iodide to form electrophilic aryl radical **A**, which undergoes 1,*n*-HAT (n = 5–7) (**A** → **B**) to afford the translocated alkyl radical at α-, β-, or γ-C(sp^3)–H sites of amines depending upon the type of tether used. The translocated palladium hybrid radical undergoes regioselective β-H loss to afford the desaturation product, either *via* radical recombination, followed by β-hydride elimination or *via* direct H-abstraction by Pd(I) species. In this report, the authors utilized the carbonyl tether for 1,5-HAT (**163a**), while using the aryl sulfonyl tether for 1,7- (**163c–d**) as well as 1,6-HAT (**163b** and **163b′**).

In the same year, Studer's group reported translocation of aryl radicals from a sulfonyl group to alkyl C–H sites (Scheme 40).[86] In this protocol, they have used thermal conditions and AIBN for radical initiation, which abstracts the weak hydrogen of tris(trimethylsilyl)silane to generate a super silyl radical, which abstracts an iodine atom from substrate **164** to generate aryl radical **A**, which undergoes 1,7-HAT at unactivated C(sp^3)–H sites of alcohols to produce **B**. The translocated nucleophilic radical undergoes radical Smiles-type rearrangement to afford remote arylated products **165a–c**.

Intermolecular HAT

In contrast to O-centered radicals,[7c,87] C-centered radicals are less efficient for intermolecular HAT. Thus, examples of intermolecular HAT by aryl radicals at C(sp^3)–H sites are scarce in the literature, mostly limited to activated C–H bonds or use of a C–H source as a solvent. HAT from tetrahydrofuran or toluene by a phenyl radical is a very fast process, with rates of 4.8×10^6 M^{-1} s^{-1} and 1.7×10^6 M^{-1} s^{-1}, respectively.[88] Due to the high reactivity of aryl radicals, other side reactions, including addition to an arene and alkene, or halogen abstraction reactions are also capable processes.

In 2005, Porta and co-workers reported a systematic study of intermolecular HAT by an aryl radical at C–H sites of tetrahydrofuran and other ethers (Scheme 41).[89] They have demonstrated that under aqueous conditions, phenyl radicals, generated from single electron reduction of diazonium salts, are able to intermolecularly abstract a hydrogen atom to form nucleophilic α-alkoxy radicals **A**. The latter adds to the *in situ* formed iminium salt **B** to afford after reduction by Ti(III) species 1,2-aminoalcohol derivatives **168a–c**.

Recently, Toste's group reported an interesting light-induced chiral diaryliodonium phosphate-mediated diastereoselective α-acetalization of cyclic ethers (Scheme 42).[90] Photochemically active diaryliodonium salt **170** is homolyzed under light irradiation to generate an aryl radical and aryl iodonium radical cation **A**; the former undergoes a regioselective intermolecular HAT with substrate **169** to produce α-alkoxy radical **B**, which then recombines with **A** to give iodonium species **C**. A subsequent elimination leads to intermediate **D** or **E**, which upon chiral diaryliodonium phosphate salt-assisted nucleophilic attack of alcohol **171** delivers the enantioenriched products **172a–b**.

More recently, Li, Zhang, Yang, Walsh and co-workers developed transition metal-free dehydrogenative cross-coupling of *N*-benzyl amines and saturated heterocycles (Scheme 43).[91] They have shown that 2-azaallyl anion **A**, generated by deprotonation of *N*-benzyl amines, can undergo SET to an aryl iodide to form an aryl radical and persistent 2-azaallyl radical **B**. The sterically protected sacrificial aryl radical undergoes intermolecular HAT at activated C(sp^3)–H sites to form stabilized nucleophilic radical **C**, which recombines with persistent 2-azaallyl radical **B** to deliver the products **174a–d**.

Conclusions

Organic radical chemistry enjoyed a prosperous period back in the 90's, which resulted in ground-breaking developments of C–H functionalization *via* the HAT pathway. Recent discoveries of mild methods for generation of radicals, which obviate the use of conventional radical initiators (*e.g.* AIBN, Et_3B) and reagents (*e.g.* Bu_3SnH, $(TMS)_3SiH$), led to a renaissance in the field, as manifested by the booming literature examples. C–H functionalization *via* HAT often distinguishes itself from transition metal-based two-electron approaches in respect of site selectivity. This complementary feature has opened up numerous opportunities to tackle longstanding problems in organic synthesis, as partially exemplified by the recent advances summarized in this review. With that being said, HAT mediated by a C-centered radical, as compared to the N- and O-centered analogues, is still underdeveloped and mostly confined to intramolecular activation. Thus, a deeper understanding of the nature and guiding parameters of reactivity is needed to harness the full potential of the C-centered radical in more challenging and complex settings, which may in turn lead to the design of novel C-centered radical precursors. Furthermore, enantioselective HAT *via* N-centered radicals has been achieved very recently,[92] thus providing the basis and motivation for the development of enantioselective HAT processes. It is

foreseeable that an asymmetric variant of C-centered radical-mediated HAT will mark a major breakthrough in this area. Undoubtedly, the progress of C-centered radical chemistry will further the field of C–H functionalization in the near future.

Conflicts of interest

The authors declare no conflicts of interest.

Acknowledgements

We thank the National Institute of Health (GM120281), National Science Foundation (CHE-1955663), and Welch Foundation (Chair, AT-0041) for financial support.

Notes and references

1 (*a*) J. Yamaguchi, A. D. Yamaguchi and K. Itami, *Angew. Chem., Int. Ed.*, 2012, **51**, 8960–9009; (*b*) J. Wencel-Delord and F. Glorius, *Nat. Chem.*, 2013, **5**, 369–375; (*c*) D. Y. K. Chen and S. W. Youn, *Chem.–Eur. J.*, 2012, **18**, 9452–9474; (*d*) T. Cernak, K. D. Dykstra, S. Tyagarajan, P. Vachal and S. W. Krska, *Chem. Soc. Rev.*, 2016, **45**, 546–576.

2 (*a*) R. G. Bergman, *Nature*, 2007, **446**, 391–393; (*b*) M. C. White, *Science*, 2012, **335**, 807–809.

3 (*a*) H. M. Davies and J. R. Manning, *Nature*, 2008, **451**, 417–424; (*b*) R. Giri, B. F. Shi, K. M. Engle, N. Maugel and J. Q. Yu, *Chem. Soc. Rev.*, 2009, **38**, 3242–3272; (*c*) T. W. Lyons and M. S. Sanford, *Chem. Rev.*, 2010, **110**, 1147–1169; (*d*) I. A. Mkhalid, J. H. Barnard, T. B. Marder, J. M. Murphy and J. F. Hartwig, *Chem. Rev.*, 2010, **110**, 890–931; (*e*) J. L. Roizen, M. E. Harvey and J. Du Bois, *Acc. Chem. Res.*, 2012, **45**, 911–922; (*f*) F. Kakiuchi and N. Chatani, *Adv. Synth. Catal.*, 2003, **345**, 1077–1101.

4 (*a*) J. M. Mayer, *Acc. Chem. Res.*, 2011, **44**, 36–46; (*b*) M. Salamone and M. Bietti, *Acc. Chem. Res.*, 2015, **48**, 2895–2903; (*c*) S. A. Green, S. W. M. Crossley, J. L. M. Matos, S. Vásquez-Céspedes, S. L. Shevick and R. A. Shenvi, *Acc. Chem. Res.*, 2018, **51**, 2628–2640; (*d*) M. Milan, M. Salamone, M. Costas and M. Bietti, *Acc. Chem. Res.*, 2018, **51**, 1984–1995.

5 J. C. K. Chu and T. Rovis, *Angew. Chem., Int. Ed.*, 2018, **57**, 62–101.

6 (*a*) A. W. Hofmann, *Chem. Ber.*, 1883, **16**, 558–560; (*b*) K. Löffler and C. Freytag, *Chem. Ber.*, 1909, **42**, 3427–3431; (*c*) D. H. R. Barton, J. M. Beaton, L. E. Geller and M. M. Pechet, *J. Am. Chem. Soc.*, 1961, **83**, 4076–4083.

7 (*a*) J. Robertson, J. Pillai and R. K. Lush, *Chem. Soc. Rev.*, 2001, **30**, 94–103; (*b*) M. Nechab, S. Mondal and M. P. Bertrand, *Chem.–Eur. J.*, 2014, **20**, 16034–16059; (*c*) L. Capaldo and D. Ravelli, *Eur. J. Org. Chem.*, 2017, **2017**, 2056–2071; (*d*) L. M. Stateman, K. M. Nakafuku and D. A. Nagib, *Synthesis*, 2018, **50**, 1569–1586; (*e*) H. Chen and S. Yu, *Org. Biomol. Chem.*, 2020, **18**, 4519–4532; (*f*) N. Goswami and D. Maiti, *Isr. J. Chem.*, 2020, **60**, 303–312; (*g*) G. Kumar, S. Pradhan and I. Chatterjee, *Chem.–Asian J.*, 2020, **15**, 651–672.

8 D. H. Hey and D. G. Turpin, *J. Chem. Soc.*, 1954, 2471–2481.

9 (*a*) D. P. Curran, D. Kim, H. T. Liu and W. Shen, *J. Am. Chem. Soc.*, 1988, **110**, 5900–5902; (*b*) D. C. Lathbury, P. J. Parsons and I. Pinto, *J. Chem. Soc., Chem. Commun.*, 1988, 81–82.

10 (*a*) M. D. E. Forbes, J. T. Patton, T. L. Myers, H. D. Maynard, D. W. Smith, G. R. Schulz and K. B. Wagener, *J. Am. Chem. Soc.*, 1992, **114**, 10978–10980; (*b*) C. Toniolo, M. Crisma, F. Formaggio and C. Peggion, *Biopolymers*, 2001, **60**, 396–419.

11 M. C. White and J. Zhao, *J. Am. Chem. Soc.*, 2018, **140**, 13988–14009.

12 W. Shu and C. Nevado, *Angew. Chem., Ind. Ed.*, 2017, **56**, 1881–1884.

13 (*a*) K. Héberger and A. Lopata, *J. Org. Chem.*, 1998, **63**, 8646–8653; (*b*) F. De Vleeschouwer, V. Van Speybroeck, M. Waroquier, P. Geerlings and F. De Proft, *Org. Lett.*, 2007, **9**, 2721–2724; (*c*) L. Jing, J. J. Nash and H. I. Kenttämaa, *J. Am. Chem. Soc.*, 2008, **130**, 17697–17709; (*d*) F. D. Vleeschouwer, V. V. Speybroeck, M. Waroquier, P. Geerlings and F. D. Proft, *J. Org. Chem.*, 2008, **73**, 9109–9120; (*e*) F. De Vleeschouwer, P. Geerlings and F. De Proft, *Theor. Chem. Acc.*, 2012, **131**, 1245; (*f*) L. R. Doming and P. Pérez, *Org. Biomol. Chem.*, 2013, **11**, 4350–4358.

14 (*a*) J. E. Bennett, B. C. Gilbert, S. Lawrence, A. C. Whitwood and A. J. Holmes, *J. Chem. Soc., Perkin Trans. 2*, 1996, 1789–1795; (*b*) D. Ravelli, M. Fagnoni, T. Fukuyama, T. Nishikawa and I. Ryu, *ACS Catal.*, 2018, **8**, 701–713.

15 (*a*) S. J. Cole, J. N. Kirwan, B. P. Roberts and C. R. Willis, *J. Chem. Soc., Perkin Trans. 1*, 1991, 103–112; (*b*) B. P. Roberts, *Chem. Soc. Rev.*, 1999, **28**, 25–35; (*c*) B. Chan, C. J. Easton and L. Radom, *J. Phys. Chem. A*, 2015, **119**, 3843–3847.

16 (*a*) X. L. Huang and J. J. Dannenberg, *J. Org. Chem.*, 1991, **56**, 5421–5424; (*b*) Y. Chen and E. Tschuikow-Roux, *J. Phys. Chem.*, 1993, **97**, 3742–3749.

17 D. Kurandina, D. Yadagiri, M. Rivas, A. Kavun, P. Chuentragool, K. Hayama and V. Gevorgyan, *J. Am. Chem. Soc.*, 2019, **141**, 8104–8109.

18 (*a*) D. J. Hart and S. C. Wu, *Tetrahedron Lett.*, 1991, **32**, 4099–4102; (*b*) S. Atarashi, J. K. Choi, D. C. Ha, D. J. Hart, D. Kuzmich, C. S. Lee, S. Ramesh and S. C. Wu, *J. Am. Chem. Soc.*, 1997, **119**, 6226–6241.

19 (*a*) J. Brunckova, D. Crich and Q. W. Yao, *Tetrahedron Lett.*, 1994, **35**, 6619–6622; (*b*) D. Crich, S. Sun and J. Brunckova, *J. Org. Chem.*, 1996, **61**, 605–615.

20 J. Cassayre and S. Z. Zard, *J. Organomet. Chem.*, 2001, **624**, 316–326.

21 M. Nechab, S. Mondal and M. P. Bertrand, *Chem.–Eur. J.*, 2014, **20**, 16034–16059.

22 (*a*) M. Tojino, Y. Uenoyama, T. Fukuyama and I. Ryu, *Chem. Commun.*, 2004, 2482–2483; (*b*) I. Ryu, T. Fukuyama, M. Tojino, Y. Uenoyama, Y. Yonamine, N. Terasoma and H. Matsubara, *Org. Biomol. Chem.*, 2011, **9**, 3780–3786.

23 M. S. Wilson, J. C. Woo and G. R. Dake, *J. Org. Chem.*, 2006, **71**, 4237–4245.

24 G. R. Dake, E. E. Fenster and B. O. Patrick, *J. Org. Chem.*, 2008, **73**, 6711–6715.
25 W. Yuan, Y. Wei, M. Shi and Y. Li, *Chem.–Eur. J.*, 2012, **18**, 1280–1285.
26 F. Scully and H. Morrison, *J. Chem. Soc., Chem. Commun.*, 1973, 529–530.
27 A. C. Pratt, *J. Chem. Soc., Chem. Commun.*, 1974, 183–184.
28 (*a*) J. M. Hornback, L. G. Mawhorter, S. E. Carlson and R. A. Bedont, *J. Org. Chem.*, 1979, **44**, 3698–3703; (*b*) J. M. Hornback and R. D. Barrows, *J. Org. Chem.*, 1982, **47**, 4285–4291.
29 T. Peez, V. Schmalz, K. Harms and U. Koert, *Org. Lett.*, 2019, **21**, 4365–4369.
30 (*a*) P. Yu, J. S. Lin, L. Li, S. C. Zheng, Y. P. Xiong, L. J. Zhao, B. Tan and X. Y. Liu, *Angew. Chem., Int. Ed.*, 2014, **53**, 11890–11894; (*b*) P. Yu, S. C. Zheng, N. Y. Yang, B. Tan and X. Y. Liu, *Angew. Chem., Int. Ed.*, 2015, **54**, 4041–4045.
31 (*a*) G. H. Lonca, D. Y. Ong, T. M. H. Tran, C. Tejo, S. Chiba and F. Gagosz, *Angew. Chem., Int. Ed.*, 2017, **56**, 11440–11444; (*b*) H. Hayashi, A. Kaga, B. Wang, F. Gagosz and S. Chiba, *Chem. Commun.*, 2018, **54**, 7535–7538; (*c*) W. Shu, E. Merino and C. Nevado, *ACS Catal.*, 2018, **8**, 6401–6406; (*d*) L. Li, H. Luo, Z. Zhao, Y. Li, Q. Zhou, J. Xu, J. Li and Y. N. Ma, *Org. Lett.*, 2019, **21**, 9228–9231.
32 (*a*) L. Huang, S. C. Zheng, B. Tan and X. Y. Liu, *Chem.–Eur. J.*, 2015, **21**, 6718–6722; (*b*) L. Huang, J. S. Lin, B. Tan and X. Y. Liu, *ACS Catal.*, 2015, **5**, 2826–2831.
33 (*a*) L. Li, L. Ye, S. F. Ni, Z. L. Li, S. Chen, Y. M. Du, X. H. Li, L. Dang and X. Y. Liu, *Org. Chem. Front.*, 2017, **4**, 2139–2146; (*b*) N. Wang, L. Ye, Z. L. Li, L. Li, Z. Li, H. X. Zhang, Z. Guo, Q. S. Gu and X. Y. Liu, *Org. Chem. Front.*, 2018, **5**, 2810–2814; (*c*) J. Zhang, W. Jin, C. Cheng and F. Luo, *Org. Biomol. Chem.*, 2018, **16**, 3876–3880; (*d*) E. P. Farney, S. S. Feng, F. Schäfers and S. E. Reisman, *J. Am. Chem. Soc.*, 2018, **140**, 1267–1270.
34 (*a*) W. Jin, Y. Zhou, Y. Zhao, Q. Ma, L. Kong and G. Zhu, *Org. Lett.*, 2018, **20**, 1435–1438; (*b*) J. H. Yang, X. B. Fu, Z. H. Lu and G. G. Zhu, *Acta Chim. Sin.*, 2019, **77**, 901–905.
35 K. J. Bian, Y. Li, K. F. Zhang, Y. He, T. R. Wu, C. Y. Wang and X. S. Wang, *Chem. Sci.*, 2020, **11**, 10437–10443.
36 P. C. Van Dort and P. L. Fuchs, *J. Org. Chem.*, 1997, **62**, 7142–7147.
37 A. Attouche, D. Urban and J. M. Beau, *Angew. Chem., Int. Ed.*, 2013, **52**, 9572–9575.
38 X. Xiao, Z. Xu, Q. D. Zeng, X. B. Chen, W. H. Ji, Y. Han, P. Wu, J. Ren and B. B. Zeng, *Chem.–Eur. J.*, 2015, **21**, 8351–8354.
39 M. Parasram, P. Chuentragool, Y. Wang, Y. Shi and V. Gevorgyan, *J. Am. Chem. Soc.*, 2017, **139**, 14857–14860.
40 For examples on unusual *endo-trig* radical cyclizations of silyl-tethered radicals due to longer Si–C and Si–O bonds, see: (*a*) M. Koreeda and L. G. Hamann, *J. Am. Chem. Soc.*, 1990, **112**, 8175–8177; (*b*) M. Parasram, V. O. Iaroshenko and V. Gevorgyan, *J. Am. Chem. Soc.*, 2014, **136**, 17926–17929.
41 For selected reviews, see: (*a*) D. Kurandina, P. Chuentragool and V. Gevorgyan, *Synthesis*, 2019, **51**, 985–1005; (*b*) P. Chuentragool, D. Kurandina and V. Gevorgyan, *Angew. Chem., Int. Ed.*, 2019, **58**, 11586–11598; (*c*) R. Kancherla, K. Muralirajan, A. Sagadevan and M. Rueping, *Trends Chem.*, 2019, **1**, 510–523; (*d*) W.-J. Zhou, G.-M. Cao, Z.-P. Zhang and D.-G. Yu, *Chem. Lett.*, 2019, **48**, 181–191; (*e*) W. M. Cheng and R. Shang, *ACS Catal.*, 2020, **10**, 9170–9196. For selected examples of alkyl Heck reaction, see: ; (*f*) D. Kurandina, M. Parasram and V. Gevorgyan, *Angew. Chem., Int. Ed.*, 2017, **56**, 14212–14216; (*g*) G. Z. Wang, R. Shang, W. M. Cheng and Y. Fu, *J. Am. Chem. Soc.*, 2017, **139**, 18307–18312; (*h*) D. Kurandina, M. Rivas, M. Radzhabov and V. Gevorgyan, *Org. Lett.*, 2018, **20**, 357–360; (*i*) M. Koy, F. Sandfort, A. Tlahuext-Aca, L. Quach, C. G. Daniliuc and F. Glorius, *Chem.–Eur. J.*, 2018, **24**, 4552–4555; (*j*) R. Kancherla, K. Muralirajan, B. Maity, C. Zhu, P. E. Krach, L. Cavallo and M. Rueping, *Angew. Chem., Int. Ed.*, 2019, **58**, 3412–3416.
42 P. Chuentragool, D. Yadagiri, T. Morita, S. Sarkar, M. Parasram, Y. Wang and V. Gevorgyan, *Angew. Chem., Int. Ed.*, 2019, **58**, 1794–1798.
43 K. Yamada, H. Fujihara, Y. Yamamoto, Y. Miwa, T. Taga and K. Tomioka, *Org. Lett.*, 2002, **4**, 3509–3511.
44 K. Yamada, Y. Yamamoto and K. Tomioka, *Org. Lett.*, 2003, **5**, 1797–1799.
45 (*a*) P. Lu, T. Hou, X. Gu and P. Li, *Org. Lett.*, 2015, **17**, 1954–1957; (*b*) T. Hou, P. Lu and P. Li, *Tetrahedron Lett.*, 2016, **57**, 2273–2276; (*c*) Y. Otake, J. D. Williams, J. A. Rincon, O. de Frutos, C. Mateos and C. O. Kappe, *Org. Biomol. Chem.*, 2019, **17**, 1384–1388.
46 C. J. Wallentin, J. D. Nguyen, P. Finkbeiner and C. R. J. Stephenson, *J. Am. Chem. Soc.*, 2012, **134**, 8875–8884.
47 (*a*) Y.-R. Luo, *Comprehensive Handbook of Chemical Bond Energies*, CRC Press, 2007; (*b*) S. J. Blanksby and G. B. Ellison, *Acc. Chem. Res.*, 2003, **36**, 255–263.
48 B. C. Gilbert and D. J. Parry, *J. Chem. Soc., Perkin Trans. 2*, 1988, 875–886.
49 F. Dénès, F. Beaufils and P. Renaud, *Synlett*, 2008, 2389–2399.
50 (*a*) U. Wille, *Chem. Rev.*, 2013, **113**, 813–853; (*b*) E. I. Heiba and R. M. Dessau, *J. Am. Chem. Soc.*, 1967, **89**, 3772–3777.
51 M. Gulea, J. M. Lopez-Romero, L. Fensterbank and M. Malacria, *Org. Lett.*, 2000, **2**, 2591–2594.
52 M. M. Logan, T. Toma, R. Thomas-Tran and J. Du Bois, *Science*, 2016, **354**, 865–869.
53 D. P. Curran and W. Shen, *J. Am. Chem. Soc.*, 1993, **115**, 6051–6059.
54 M. Ratushnyy, M. Parasram, Y. Wang and V. Gevorgyan, *Angew. Chem., Int. Ed.*, 2018, **57**, 2712–2715.
55 E.-A. I. Heiba and R. M. Dessau, *J. Am. Chem. Soc.*, 1967, **89**, 3772–3777.
56 E. Bosch and M. D. Bachi, *J. Org. Chem.*, 1993, **58**, 5581–5582.
57 S. Bogen, M. Gulea, L. Fensterbank and M. Malacria, *J. Org. Chem.*, 1999, **64**, 4920–4925.
58 R. Bénéteau, C. F. Despiau, J. C. Rouaud, A. Boussonnière, V. Silvestre, J. Lebreton and F. Dénés, *Chem.–Eur. J.*, 2015, **21**, 11378–11386.
59 (*a*) S. Wu, X. Wu, D. Wang and C. Zhu, *Angew. Chem., Int. Ed.*, 2019, **58**, 1499–1503; (*b*) S. Yang, X. Wu, S. Wu and C. Zhu, *Org. Lett.*, 2019, **21**, 4837–4841.

60 (*a*) T. Shang, J. Zhang, Y. Zhang, F. Zhang, X. S. Li and G. Zhu, *Org. Lett.*, 2020, **22**, 3667–3672; (*b*) Z. Xiong, F. Zhang, Y. Yu, Z. Tan and G. Zhu, *Org. Lett.*, 2020, **22**, 4088–4092.
61 H. Li, L. Guo, X. L. Feng, L. P. Huo, S. Q. Zhu and L. L. Chu, *Chem. Sci.*, 2020, **11**, 4904–4910.
62 P. Devin, L. Fensterbank and M. Malacria, *J. Org. Chem.*, 1998, **63**, 6764–6765.
63 G. M. Allan, A. F. Parsons and J. F. Pons, *Synlett*, 2002, 1431–1434.
64 H. Lin, A. Schall and O. Reiser, *Synlett*, 2005, 2603–2606.
65 S. K. Pagire and O. Reiser, *Green Chem.*, 2017, **19**, 1721–1725.
66 (*a*) J. K. Vellucci and C. M. Beaudry, *Org. Lett.*, 2015, **17**, 4558–4560; (*b*) R. Kim, A. J. Ferreira and C. M. Beaudry, *Angew. Chem., Int. Ed.*, 2019, **58**, 12595–12598.
67 Y. Yoshimura, Y. Yamazaki, K. Wachi, S. Satoh and H. Takahata, *Synlett*, 2007, 111–114.
68 (*a*) A. H. Lewin, A. H. Dinwoodie and T. Cohen, *Tetrahedron*, 1966, **22**, 1527–1537; (*b*) T. Cohen, C. H. McMullen and K. Smith, *J. Am. Chem. Soc.*, 1968, **90**, 6866–6867.
69 S. H. Pines, R. M. Purick, R. A. Reamer and G. Gal, *J. Org. Chem.*, 1978, **43**, 1337–1342.
70 D. P. Curran and J. Xu, *J. Am. Chem. Soc.*, 1996, **118**, 3142–3147.
71 D. P. Curran and H. S. Yu, *Synthesis*, 1992, 123–127.
72 (*a*) V. Snieckus, J. C. Cuevas, C. P. Sloan, H. T. Liu and D. P. Curran, *J. Am. Chem. Soc.*, 1990, **112**, 896–898; (*b*) D. P. Curran and H. T. Liu, *J. Chem. Soc., Perkin Trans. 1*, 1994, 1377–1393; (*c*) D. P. Curran, A. C. Abraham and H. T. Liu, *J. Org. Chem.*, 1991, **56**, 4335–4337; (*d*) D. P. Curran, H. S. Yu and H. T. Liu, *Tetrahedron*, 1994, **50**, 7343–7366.
73 M. Parasram, P. Chuentragool, D. Sarkar and V. Gevorgyan, *J. Am. Chem. Soc.*, 2016, **138**, 6340–6343.
74 G. H. Han, M. C. Mcintosh and S. M. Weinreb, *Tetrahedron Lett.*, 1994, **35**, 5813–5816.
75 F.-Q. Huang, X. Dong, L.-W. Qi and B. Zhang, *Tetrahedron Lett.*, 2016, **57**, 1600–1604.
76 P. Liu, J. Tang and X. Zeng, *Org. Lett.*, 2016, **18**, 5536–5539.
77 (*a*) W. C. Wertjes, L. C. Wolfe, P. J. Waller and D. Kalyani, *Org. Lett.*, 2013, **15**, 5986–5989; (*b*) W. C. Wertjes, P. J. Waller, K. E. Shelton and D. Kalyani, *Synthesis*, 2014, **46**, 3033–3040.
78 B. S. Bhakuni, A. Yadav, S. Kumar, S. Patel, S. Sharma and S. Kumar, *J. Org. Chem.*, 2014, **79**, 2944–2954.
79 J. Q. Chen, Y. L. Wei, G. Q. Xu, Y. M. Liang and P. F. Xu, *Chem. Commun.*, 2016, **52**, 6455–6458.
80 M. Ratushnyy, N. Kvasovs, S. Sarkar and V. Gevorgyan, *Angew. Chem., Int. Ed.*, 2020, **59**, 10316–10320.
81 H. Tian, H. Yang, C. Zhu and H. Fu, *Sci. Rep.*, 2016, **6**, 19931.
82 S. Du, E. A. Kimball and J. R. Ragains, *Org. Lett.*, 2017, **19**, 5553–5556.
83 A. F. Voica, A. Mendoza, W. R. Gutekunst, J. O. Fraga and P. S. Baran, *Nat. Chem.*, 2012, **4**, 629–635.
84 K. A. Hollister, E. S. Conner, M. L. Spell, K. Deveaux, L. Maneval, M. W. Beal and J. R. Ragains, *Angew. Chem., Int. Ed.*, 2015, **54**, 7837–7841.
85 P. Chuentragool, M. Parasram, Y. Shi and V. Gevorgyan, *J. Am. Chem. Soc.*, 2018, **140**, 2465–2468.
86 F. W. Friese, C. Muck-Lichtenfeld and A. Studer, *Nat. Commun.*, 2018, **9**, 2808.
87 (*a*) K. A. Margrey, W. L. Czaplyski, D. A. Nicewicz and E. J. Alexanian, *J. Am. Chem. Soc.*, 2018, **140**, 4213–4217; (*b*) A. Hu, J.-J. Guo, H. Pan and Z. Zuo, *Science*, 2018, **361**, 668–672; (*c*) S. Mukherjee, B. Maji, A. Tlahuext-Aca and F. Glorius, *J. Am. Chem. Soc.*, 2016, **138**, 16200–16203.
88 J. C. Scaiano and L. C. Stewart, *J. Am. Chem. Soc.*, 1983, **105**, 3609–3614.
89 A. Clerici, R. Cannella, W. Panzeri, N. Pastori, E. Regolini and O. Porta, *Tetrahedron Lett.*, 2005, **46**, 8351–8354.
90 B. Ye, J. Zhao, K. Zhao, J. M. McKenna and F. D. Toste, *J. Am. Chem. Soc.*, 2018, **140**, 8350–8356.
91 Z. Liu, M. Li, G. Deng, W. Wei, P. Feng, Q. Zi, T. Li, H. Zhang, X. Yang and P. J. Walsh, *Chem. Sci.*, 2020, **11**, 7619–7625.
92 K. M. Nakafuku, Z. Zhang, E. A. Wappes, L. M. Stateman, A. D. Chen and D. A. Nagib, *Nat. Chem.*, 2020, **12**, 697–704.